Dear Editor,

We hereby submit our reply to the three reviews on our manuscript, “Greenland ice velocity maps from the PROMICE project” by Solgaard et al.

In the following, we provide a point-by-point response to all the reviewer comments. The reviewer comments are in black while our replies are in green using a different font for clarity. A tracked changes version of the manuscript is included.

We have followed all suggestions in the reviewers’ general comments except one. Reviewer #3 suggests that we compare our velocity products against other already available satellite-derived velocities. While this is a worthwhile exercise which would be of interest to the large community of users, we find that it is out of scope for our manuscript. We have performed a thorough validation of our product using available in-situ GPS observations and as suggested by both Reviewer #1 and #2 included an analysis of pixels covering stable ground. Both analyses as well as the study by Hvidberg et al, 2020 show that the PROMICE product performs as expected.

We thank the editor and all three reviewers for useful and constructive feedback and comments.

Sincerely,

Anne Solgaard on behalf of all co-authors.

REVIEWER 1

Review of “Greenland ice velocity maps from the PROMICE project” by Anne Solgaard et al.
This manuscript entitled “Greenland ice velocity maps from the PROMICE project” generates a time series of Greenland Ice Sheet (GIS) velocity mosaic spanning from September 2016 to present with a high temporal resolution of 24 days and a spatial resolution of 500 m based on the Sentinel-1 SAR data. In the main text, the authors introduced the data processing steps (e.g., how to extract the ice velocity and how to perform the data fusion) and the relevant error analysis (e.g., regarding the orbit error, geolocation bias correction, ionospheric effects etc.) and the validation of the results (by comparison with the in-situ GPS measurements) in detail. Overall, this manuscript was well written and organized, and the produced dataset is reliable and acceptable. And the reviewer believes that the dataset will largely contribute to the understanding of GIS ice dynamics and the behind mechanism of accelerated mass loss. Hence, this manuscript can be accepted once some issues listed below are addressed.

General comments:

1.With regard to the extraction of the glacier velocity when using the offset-tracking technique, the issue of how to perform the co-registration for huge amounts of SAR data, which is the most important steps for remote sensing data processing, is left out. Please clarify relevant issues, and a more detailed description is preferred.

No resampling is carried out to coregister the images, for several reasons:

(a) The ice motion is spatially variant, and can represent several pixels of displacement. To coregister accurately, it would thus have to be known a priori, but since the displacement is the quantity we wish to measure, this is not feasible.
(b) Intensity cross-correlation does not rely on the complex image phase, and employs large windows (256x64 in this case), therefore subpixel resampling of the images is not necessary. Instead we just extract patches in the images centered on integer pixel locations, computed based on precise state vectors and on the acquisition geometry, and correct subsequently for the fractional pixel shift.

We have revised section 4.2, and added the following clarification regarding coregistration:
“For intensity cross-correlation methods, the SLCs need not be coregistered and resampled to sub-pixel accuracy prior to the processing, as they rely on relatively large windows (several tens of pixels in each dimension). Instead, for the regular grid points in the reference SLC, we calculate the expected position of the corresponding grid points (assuming no motion) in the second SLC, based solely on SLC timing information, orbital state vectors, and the DEM. The grid points are selected on integer pixel positions in the reference SLC, but the corresponding grid points will generally not coincide with integer pixel locations in the second SLC. To avoid resampling the second SLC, we round the corresponding grid points

to their nearest integer pixel locations and save the fractional shifts, which are then added back to the offset measurement after cross-correlation."

2.For the error assessment of the final glacier velocity dataset, the offsets in ice-free areas are generally evaluated and discussed. However, this manuscript did not give relevant explanations and discussions. This information needs to be further described.

Yes, we completely agree. This important measure of product performance. We have carried out an analysis of all ice free pixels in all the mosaics of the PROMICE product (more than $142 \cdot 10^6$ points). This analysis gives:

	vmag	vx	Vy
STD	9.8 m/yr	7.7 m/yr	11.9 m/yr
Mean of all points	10.2 m/yr	0.1 m/yr	-0.6 m/yr
# of points	142710462	142710462	142710462

We have inserted a paragraph following the validation against GPS describing the analysis of stable ground pixels in Section 7: Validation:

'We perform a similar analysis for the PROMICE product for the pixels over stable ground, where no movement is expected.All pixels on ice-free terrain from all mosaics (each spanning 24 days) in the time series are included, which totals to more than $142 \cdot 10^6$ points. The resulting values of the standard deviation and bias 8 m/yr and 0.09 m/yr for the v_x-component and 12 m/yr and -0.6 m/yr for the v_y-component, respectively (see Tab. 6). The values of the standard deviation are less than half the values of the validation against GPS measurements, while the biases are significantly lower (in absolute value) and thus closer to zero. In this analysis, the standard deviation and bias are also largest for the v_y-component as discussed above.'

A table has also been included for comparison to the validation using GPS-observations: Table 6:

Product	Magnitude		x-dir		y-dir	
	Std [m/yr]	Bias [m/yr]	Std [m/yr]	Bias [m/yr]	Std [m/yr]	Bias [m/yr]
PROMICE Product (All pairs)	10	10	8	0.1	12	-0.6

3.Some issues with respect to the formatting and written need to be revised, please see the specific comments.

Specific comments:

P1: In the abstract, after the location of the website, the authors added the references (Solgaard and Kusk, 2021), which corresponds to the content of this manuscript. Please confirm if this is OK?

We confirm this. The DOI and dataset citation is included in accordance with the manuscript guidelines:

1. Abstract: the abstract should be intelligible to the general reader without reference to the text. After a brief introduction of the topic, the summary recapitulates the key points of the article and mentions possible directions for prospective research. Reference citations should not be included in this section (except for data sets) and abbreviations should not be included without explanations. At least for the final accepted publication, a functional data set DOI and its in-text citation must be given in the abstract. If multiple data set DOIs are necessary, please instead refer to the data availability section.

P1, L9: Suggest that using the phrases “north-south direction” and “east-west direction” replaces the Vx and Vy.

Agree, this makes good sense in the abstract. It now reads:
‘...for the components in the eastern and northern direction, respectively.’

P4, L4-6: The “Fig. 2A” and “Fig. 2B” should be changed to “Fig. 2a” and “Fig. 2b”, respectively.

Done

P4, L4-6: Changing the phrase “See 5” to “See section 5” seems to be better. There are several errors of this type in the main text, please check and fix them.

They are fixed.

P5, L7-8: More information about the GIMP DEM is needed.

We have added:

‘We employ the Greenland Ice Mapping Project (GIMP) DEM based on the ASTER and SPOT 5 DEMs and AVHRR photoclinometry (Howat et al., 2014, 2015), downsampled to 500 m spacing to match the resolution of the IV product.’

And included the missing dataset reference: Howat et al., 2015.

P5, L10: Does the term (“TPP”) have a full name? if so, please clarify.

We have added:

“The data processing is carried out using the Interferometric Post Processing (IPP) processor, developed and maintained by DTU Space \citep{Kusk2018}. Despite the name, the processor also performs offset-tracking for displacement measurements, which is the functionality used to generate the PROMICE product”

P6: For the flow chart (i.e., Fig.3), it is just a simple and conventional description for the data processing of this study. The reviewer suggests that more detailed processes of data processing should be given in this figure. In addition, add the item related to the data co-registration.

The figure has been split in two sub-figures, with figure b showing a detailed flow diagram of the offset-tracking.

P6, L7-9: Please add the word “section” to these expressions like “in 4.2”, “in 4.3 and 5”, “in 4.4”.

This has been fixed.

P7: For the section 4.2 (“Offset-tracking”), please add and clarify the issue of how to perform data co-registration (more information needs to be given), which is one of the most important procedures when employing the offset-tracking technique to extract the glacier velocity. In particular, for the constantly updated data, how to deal with?

This is addressed above in the answer to the first comment.

P10, L15: This expression like “the range standard deviation” can easily be misunderstood. So a more clear expression like “the standard deviation in range direction” would be better. Similar issues can also be seen in Table 2, e.g., “Rang is line of sight and azimuth is along the satellite flight path”.

Agreed. We have changed the paragraph as the following

“We note that the range velocity bias (-0.5~m/yr) and azimuth velocity bias (0.5~m/yr) do not differ between the precise and the restituted orbit files. The standard deviation in the range direction is 2.7~m/yr for the precise orbit files and 2.8~m/yr for the restituted orbit files, while the standard deviation in the azimuth direction is 3.3~m/yr for both orbit types.”

The caption for Table 2 has been corrected to “Range direction is line of sight and azimuth direction is along the satellite flight path”. The headings in the Table have, for clarification, also been changed to “Range Velocity Bias / Range Velocity Std/ Azimuth Velocity Bias/Azimuth Velocity Std”

P13, L8: Please confirm if the units are correct? (9.7 m/s and 24.4 m/s?)

This was indeed a typo. The units have been changed to m/yr.

P15, L8-10: From the magnitude of the error (up to 300 m/a) caused by ionospheric effects, this item is the most significant uncertainty source. Why didn’t the authors try to apply the relevant

methods mentioned in last paragraph? The reviewer thinks that developing a better or targeted method is necessary, as the author also mentioned that the post-processing step did not completely eliminate this type of error.

The ionospheric effects are indeed the major error source, and we have experimented with methods relying on the dispersive properties of the ionosphere, similar to the ones described in (Gomba 2018) and (Liao et. al., 2018). However for Sentinel-1 level 1 products, there is a problem with block processing artifacts present in most Sentinel-1 SLCs, which severely hampers this approach. Another method to reduce the impact of ionospheric effects is to exploit the fact that in some regions, measurements from both ascending and descending tracks are available, and in this case one can derive the horizontal velocity from only the range offsets, which are much less affected by the ionosphere. This is being worked on, and will be included in a future update of the processor. We have added the following text:

"Another method to reduce the impact of ionospheric effects is to exploit the fact that in some regions, measurements from both ascending and descending tracks are available, and in this case, ice velocities can be derived from only the range offsets -- which are much less sensitive to ionospheric effects -- and the SPF assumption(see Sect.4.3). In the standard S1 acquisition plan (Fig. 2a), only two ascending tracks are acquired (the long track along the west coast of Greenland, and the track covering the northeast margin of the ice sheet up to the northernmost point), so the method will not be applicable everywhere. During the winter campaigns ((Fig. 2b), this method will be applicable in a much larger part of the ice sheet. Work is undergoing to include this method in a future update of the PROMICE product."

P15: In the section 5.5, when it comes to the error assessments, a common method of calculating the offsets over the ice-free areas is usually adopted and further analyzed. So relevant information regarding the results of ice-free areas deserved to be given.

We agree on this. Please see our response to comment nr.2 under General Comments. We have inserted a stable ground analysis in Section 7: Validation following the paragraphs on validation against GPS observations.

P15, L16-17: Providing a clear explanation regarding the correct magnitude of the errors seems to be better, now that you mentioned the study of Boncori et al. (2018). Moreover, the format of the reference "in (Boncori et al., 2018)" can be changed to "in Boncori et al. (2018)". Please check.

The reference format has been corrected.

P16: To ensure the consistency in writing, the word "Primice" in the subtitle should be changed to "PRIMICE".

Agree, done.

P17, L4-6: Please add the position information about the Melville Bay and Scoresbysund areas in Fig. 2.

We have added the locations of the areas discussed in Section 6 on Figure 10 and added a reference to the figure at the position in text. We used Figure 10 rather than Figure 2, because it is closer to the discussion in the manuscript.

P23: For the Fig. 12 (also for Fig. 4), a revised figure with higher resolution is needed. Now it looks a little fuzzy.

We have added less transparent grid lines to Figure 12 and increased the font size on the axes making it less fuzzy. The resolution of Figure 4 has been increased and the position of the grounding line has been added.

REVIEWER 2: Ben Davison

General comments

The PROMICE ice velocity product represents a significant improvement on existing operational Greenland Ice Sheet velocity products, particularly in terms of temporal resolution and timeliness. Indeed, the community has no doubt already benefitted substantially from this product and will continue to do so in future. With that in mind, this paper is an important source of documentation for what is, and will continue to be, a widely used product; therefore, it is crucial that the paper is clear and thorough throughout.

This paper presents a detailed description of the PROMICE ice velocity product and the operational processing chain used to produce it. The paper is (in most places) clear, detailed and thorough: it includes clear and accurate descriptions of each processing stage, error sources and estimation, validation, as well as the product itself. Whilst there are no major issues with the paper, I felt that some sections would benefit from more detail (or alternative descriptions) and, particularly in the second half of the manuscript, the writing lost some of the precision and concision found in the first half of the manuscript. I also have some suggestions that I believe will improve the clarity of the figures and associated descriptions. With these changes and suggestions implemented, I would be happy to recommend the manuscript for publication in this journal.

Below, I provide more specific comments, going through the paper line by line:

Page 1, line 7: when describing the GPS validation in the abstract, I think it would be beneficial to also provide the biases, and perhaps also the uncertainty estimation from velocity estimates over bedrock, because both are useful measures and ones which many readers will be familiar with.

Agree. We have carried out the analyses over stable ground and include the results in the abstract along with values for the bias (also for the validation with GPS):

'The product is validated against in-situ GPS measurements. We find that the standard deviation of the difference between satellite and GPS derived velocities (and bias) is 20 m/yr (-3 m/yr) and 27 m/yr (-2 m/yr) for the components in the eastern and northern direction, respectively. Over stable ground the values are: 8 m/yr (0.1 m/yr) and 12 m/yr (-0.6 m/yr) in the eastern and northern direction, respectively.'

We also include the analysis over stable ground in the validation section. See our response to Reviewer #1's General Comment #2.

Page 1, line 9: would 'east-west and north-south' be clearer than 'vx and vy' at this stage

in the manuscript?

Yes, this makes more sense in the abstract. See wording in the response to your previous comment.

Page 1, line 11: By 'excellent data coverage', do you mean comprehensive/complete imaging of the ice sheet by Sentinel-1? I realise that's a bit more clunky, but could you be more specific here?

Yes, it is more precise. The text now reads:
'Best spatial coverage is achieved in winter due to the comprehensive data coverage by Sentinel-1 and high coherence, while summer mosaics have the lowest coverage due to widespread melt.'

Page 1, line 14: 'and dynamics of glaciers' - can you add a timescale here? Such as '…over seasonal and longer timescales' (as discussed in the conclusion).

Yes, the last line now reads:
''The spatial comprehensiveness and temporal consistency make the product ideal for both monitoring and for studying ice-sheet wide ice discharge and dynamics of glaciers on seasonal scales.'

Page 1, line 18: I'd suggest that 'obtain ice sheet-wide observations of ice-flow velocities' makes an even stronger case for the product.

Agree, 'ice-sheet wide' is now included.

Page 1, line 22: Can you add 'tidewater glacier' before 'ice-flow velocities'? I assume this is the intended focus given the introduction on sea level rise and the reference (Ahlstrom et al., 2013). Alternatively, it would be worth also referencing one or two of the GPS studies carried out on land-terminating sectors.

We wanted to highlight that there just are not very many in-situ measurements of ice flow and especially not long term ones. We thus agree that the old wording was not clear on this, we have included references to more in-situ observations and changed the wording:

'In-situ measurements of ice-flow velocities are relatively sparse on the GrIS and most of the measurements stem from GPS surveys (Ahlstrøm et al., 2013).'
->
'In-situ measurements of ice-flow velocities (e.g. from GPS) are relatively sparse on the GrIS and are often of short duration (months) at high temporal resolution (e.g. Sole et al., 2011; Maier et al., 2019) or of longer duration (years) but at low temporal resolution (e.g. Thomas et al., 1998; Hvidberg et al., 2020) while few span several years at high temporal resolution (e.g. Ahlstrøm et al., 2013). '

Page 1, line 23: I suggest 'inaccessibility and size of the GrIS, as well as the harsh…'. Alternatively, a subsequent sentence stating that the size of the GrIS makes it impractical

to obtain continuous measurements of the whole ice sheet through field observations.

Yes, this is an important point. We go with your first suggestion.

Page 2, line 3: 'IV' doesn't seem to be used in preference to 'ice velocity' throughout the manuscript. I don't have a strong preference for either, but perhaps just stick to ice velocity for simplicity?

Yes, the abbreviation is unnecessary in the paper. We stick to 'ice velocity' throughout.

Page 2, line 28: The statement about weighted averaging is repeated a few lines later – perhaps it could be removed from one of the two sentences?

Agreed. The first occurrence has been changed to "each mosaic is based on velocity measurements from all possible 6- and 12-day pairs".

Page 4, line 2: I wonder if it would be worth providing the pixel spacing (2.3x14.1 m) as well as the resolution here? This would help maintain consistency with the description of the output grid dimensions in section 4.2, which seem to be based on pixel spacing.

This is correct, we have added "The pixel spacing of the product is 2.3 m in slant range, and 14.1 m in azimuth."

Page 4, line 20: Isn't stripmap mode higher resolution?

Yes, this is correct, the reference to product type here refers to the processing type (SLC/GRD/…), with IW acquisition mode implied. We have rephrased to "the highest resolution of the available IW product types".

/(check which resolution of DEM: Use GIMPdem90m) Page 5, line 8: Is the DEM downsampled before calculating the vertical component of ice
displacement? If so, I think it would be worth quantifying how this affects your vertical displacement estimate.

The DEM, when used for deriving the surface gradient in the surface parallel flow approximation, should approximately match the resolution of the offset maps, in order to avoid aliasing of high frequency slope variation. We have added the following to section 4.3:
"The effective resolution of the velocity maps is on the order of the correlation window size, which corresponds to approximately 800×900 m on ground (see Sect. 4.2), so the resolution of the surface gradient map should approximately match this. The DEM is downsampled to the pixel spacing of the PROMICE product (500×500 m), and the gradient is derived using second order differences, which means the gradients are derived using samples approximately 1000 m apart."

Page 6: The need to focus SAR images is mentioned briefly in the discussion, but I can't see any description of how the SAR images were focused, which should acknowledge the difficulties associated with TOPS mode data.

Focusing TOPS images is indeed tricky, which is why we use the SLC product, which is delivered focused by ESA using the Sentinel-1 Instrument Processing Facility (IPF). We have emphasised in Section 2.3 that the SLC images are already delivered as focused SAR images.

Page 7, lines 10-15: Was there any filtering of the intensity images prior to crosscorrelation to e.g. minimise the visibility of long-wavelength features, or to enhance the contrast in the images? I've found it increases the signal to noise ratio in my own, much smaller scale, investigations.

We do not apply a high-pass filter. The use of such filters are described in (deLange,2007), where it is applied successfully to intensity tracking on outlet glaciers. It is definitely of interest to us, but It is not clear, however, that it would be beneficial in the interior, where the offset-tracking relies on the presence of speckle, rather than features, or that the same filter parameters would be optimal everywhere. For the operational PROMICE product, where a manual fine-tuning is not feasible, we currently choose not to rely too much on adaptive, data-dependent processing, in order to have a consistent product.

Page 7, lines 10-15: I think it would be worth mentioning here that several techniques that are often used to co-register Sentinel 1 images fail over moving ice (such as crosscorrelation or Enhanced Spectral Diversity) fail because they rely on stationary surfaces, and so you have to rely on the orbit information and DEM.

Yes, this is indeed correct. We have addressed this also in an answer to reviewer 1, which I repeat below:
No resampling is carried out to coregister the images, for several reasons:

(c) The ice motion is spatially variant, and can represent several pixels of displacement. To coregister accurately, it would thus have to be known a priori, but since the displacement is the quantity we wish to measure, this is not feasible.
(d) Intensity cross-correlation does not rely on the complex image phase, and employs large windows (256x64 in this case), therefore subpixel resampling of the images is not necessary. Instead we just extract patches in the images centered on integer pixel locations and correct subsequently for the fractional pixel shift.

We have revised section 4.2, and added the following clarification regarding coregistration:
"For intensity cross-correlation methods, the SLCs need not be coregistered and resampled to sub-pixel accuracy prior to the processing, as it relies on relatively large windows (several tens of pixels in each dimension). Instead, for the regular grid points in the reference SLC, we calculate the expected position of the corresponding grid points (assuming no motion) in the second SLC, based solely on SLC timing information, orbital state vectors, and the DEM. The grid points are selected on integer pixel positions in the reference SLC, but the corresponding grid points will generally not coincide with integer pixel

locations in the second SLC. To avoid resampling the second SLC, we round the corresponding grid points to their nearest integer pixel locations and save the fractional shifts, to be added back to the shift measurement after cross-correlation."

Page 7, line 23: 'local medians' – can you specify what data this relates to? (i.e. velocity, flow direction etc)

The approach is applied independently to the range and azimuth velocities. We have included a expanded description of the approach:
"Then, a further culling, is carried out on the on the range and azimuth shifts, using a normalized median test, as described in (Westerweel and Scarano, 2005).For each measurement,U_0, in a 5×5 neighbourhood, the median,U_m, of the 24 surrounding measurements($U_1,U_2,...,U_{25}$) is calculated (excluding U_0), and for each measurement in the neighbourhood, a residual,$R_i=|U_i-U_m|$is calculated. The median,R_m, of($R_1,R_2,...,R_{24}$) is then calculated, and used to normalize the residual ofU_0 so that $R_{m'}=|U_0-U_m|/(R_m+\epsilon)$,where ϵ is a minimum normalization level that accounts for cross-correlation noise. We use ϵ= 0.1 pixel, as suggested in(Westerweel and Scarano, 2005), and cull the measurement,U_0, if R'_0 exceeds a threshold of 5 for either of the range or azimuth shifts. This value was found by experiments to remove most clearly visible outliers, without removing valid measurements.Lower values removed more outliers, but had an adverse effect on measurement coverage"

Page 7, line 24: I wonder if these outliers due to surface melt could be removed using a 'dusting' approach as in Selley et al (2021), or using a region growing approach as in Luttig et al. (2017)

Luttig, C., Neckel, N., and Humbert, A. 2017. A combined approach for filtering ice surface velocity fields derived from remote sensing methods. Remote Sensing, 9(10). DOI: https://doi.org/10.3390/rs9101062

Selley, H. L., et al. 2021. Widespread increase in dynamic imbalance in the Getz region of Antarctica from 1994 to 2018. Nature Communications, 1133. DOI: https://doi.org/10.1038/s41467-021-21321-1.

We believe the approach described in the answer to the previous question, in combination with the temporal culling of the final velocity maps, is very similar to the "dusting" approach described in (Selley, et.al., 2021). Like them, we also remove small unconnected segments of pixels in each offset map prior to fusion, as these tend to be unreliable. We have added the following sentence to Sect.4.2, after the expanded description of the median-based culling approach:
"After the culling, small unconnected segments of pixels (<25 pixels) are removed, as these were found to often contain erroneous values."

Page 7, last line: Is this technically a resampling? I thought it was actually a scattered interpolation, because the ground-surface pixel size varies throughout the image.

This is indeed a scattered interpolation. The definition of resampling seems to differ between various fields; in SAR literature, the term resampling is often used also for the irregular interpolation in slant-to-ground range conversion and geocoding. For clarity, we have changed the term “resampled” to “interpolated”

Page 8, section 4.4: When fusing velocity estimates from both 6- and 12-day pairs to generate the 24-day mosaics, are the different time periods considered? And how? I imagine you could interpolate them both to daily values and weight them accordingly.

This is described in section 4.3: “The shifts and standard deviations are converted to velocity by multiplying with the SLC pixel spacing and dividing by the temporal baseline”. As the standard deviations (in the form of the inverse of the variances) are used to weight the measurements in the fusion (Eq. 3), this accounts for the varying temporal baselines.

Page 10, line 2: ‘knowledge’ seems an odd word to use here. Perhaps ‘accuracy’ would be better?

We have changed the sentence to. “Errors in the Sentinel-1 orbital state vectors provided by ESA, …”

Page 10, lines 4-6: It looks like these error estimates assume that the orbital errors apply to only one of the images. I think if you assume a 5 cm error in both images, these velocity errors would double? Since the product used the restituted orbits, I think it would also be more appropriate to frame these sentences in terms of the 10 cm accuracy of those data, even though your investigation shows that the measured errors are very similar for both of them.

It is correct that we should account for the error on both images. Since the values are given as RMS the errors on the displacement should be multiplied by $\sqrt{2}$. We have rewritten the paragraph using the values for the restituted orbits and applied the factor of $\sqrt{2}$:

“For Sentinel-1 data, absolute orbital errors are on the order of 5 cm RMS when using the precise orbit product available after 21 days (Peter et al., 2017). The restituted orbits typically used in the PROMICE product generation are available shortly after acquisition, and have a nominal accuracy of 10 cm RMS. This corresponds to 8.6 m/yr RMS for a velocity measurement using a 6-day pair and 4.3 m/yr for a 12-day pair.”

Page 13, line 9: I’m a bit confused by the use of ‘delays’ because the timing aspect hasn’t been introduced yet as far as I can tell. Would ‘shifts’ be appropriate, since it’s used in the previous sentence?

Agreed, “shifts” is more appropriate. We have changed the text.

Page 13, line 18: ‘affecting the ability to measure ice velocity’: can you be more specific here and relate this to the cross-correlation procedure?

We have changed the sentence to:
"Temporal decorrelation is caused by changes in radar backscatter between acquisitions that reduce the correlation between the image patches which are cross-correlated in the offset-tracking procedure, leading to noisy or even missing measurements."

Page 13, line 21: 'sub-resolution structure' of the snow/ice?
In this case yes, but more generally, the sub-resolution structure of the imaged scene. We have changed the sentence to:
"*Speckle is a property of radar images, caused by variations in the sub-resolution structure of the imaged scene,"*

Page 13, line 23: I think that 'If the scene is moving…. From the same track' is perhaps unnecessary and it would be sufficient just to say speckle can be used to track ice flow when the ice-flow is spatially uniform over the dimensions of the interrogation areas.
It is important that the track is repeated with sufficient precision, since large spatial baselines can also degrade the coherence, although for Sentinel-1 this is generally not a problem due to the tight orbital tube. We have rephrased to:
"If the ice-flow is spatially uniform and the sensor track does not deviate excessively for the two acquistions (the latter is generally not a problem for Sentinel-1), the speckle pattern can be tracked between acquisitions"

Page 13, line 24: perhaps 'steep spatial gradients in ice flow', or similar, rather than just 'rapid ice flow'.
Agree, we have changed "rapid ice flow" to "steep spatial gradients in ice flow".

Page 13, line 25: 'the noise level exceeds the signal' is a bit confusing (and impossible by definition?). Perhaps 'the signal to noise ratio is low' would be sufficient?
Page 13, lines 25-26: 'by averaging multiple measurements to reduce the noise' – can you specify what you mean by measurements in this context? Multiple shift maps in the mosaic? Or spatially over multiple pixels?
We have changed the wording to:
"Often in the interior, the signal-to-noise ratio is low, but since up to five velocity maps from each track are averaged to produce the PROMICE product, the noise can be reduced."

Page 13, line 28: It's not clear what the difference between 'noisy' and 'patchy' is in this context. Would one or the other suffice?
This is correct, from the preceding discussion it is implicit that the measurements are noisy. We have changed the wording to:
"In extended homogeneous areas of low coherence, the velocity measurements can become patchy, since many unreliable measurements will be discarded by the culling procedures"

Page 15, line 4: We have used a variational stationary noise filter to good effect to remove ionospheric striping in the velocity estimates. The method we applied to the Sentinel 1 velocity estimates is described very briefly in Tuckett et al. (2019), and the underlying algorithm is described in Fehrenbach et al. (2012). I think the code is documented here: https://www.math.univtoulouse.fr/~weiss/Codes/VSNR/VNSR_VariationalStationaryNoiseRemover.html

Fehrenbach, J., Weiss, P., and Lorenzo, C. 2012. Variational algorithms to remove stationary noise: applications to microscopy imaging. IEEE Transactions on Image Processing. DOI: 10.1109/TIP.2012.2206037.

Tuckett, P. A., Ely, J. C., Sole, A. J., Livingstone, S. J., Davison, B. J., van Wessem, M., Howard, J. 2019. Rapid accelerations of Antarctic Peninsula glaciers driven by surface melt. Nature Communications, 10, 4311. DOI: https://doi.org/10.1038/s41467-019-12039-2.

This is an interesting approach, and something for us to look into, although its performance should be assessed in the typical case where there can be quite a lot of missing data in the individual pairs.

Page 17, line 2: See my comment re Figure 10. Perhaps referring to regions or low/high coverage, rather than regions of blue/yellow in Figure 10 would be clearer?

Yes it makes more sense -we have changed the wording accordingly. See also our response to your comment on Figure 10.

Page 17, line 8: Can you clarify what you mean by 'amount of data'?

Yes, 'amount of data' is changed to 'number of acquisitions'.

Page 19, line 2: 'properties observed by the radar' is a bit vague. Can you be more specific here, for example by referring to coherence or speckle?

Yes, it now reads: '..-both processes leading to loss of coherence.'

Page 19, line 6: It's not clear to me what this means – does it mean high standard deviation in the velocity maps? Or some other measurement of uncertainty?

We have deleted this sentence. It is more confusing than informative.

Page 21, lines 21-22: 'outer most parts of the outlet glaciers still have reasonable coverage' is a little vague. Can you clarify what you mean by 'outer'? And by 'reasonable' do you mean that it is better than the 2-cycle PROMICE product?

Agreed this part is a little vague. What we mean is that when increasing the temporal resolution there is still data (although with increased noise) on the outlet glaciers -it mainly the ablation areas with lower flow speeds that are affected. We have changed the wording -see below. See also our response to your comment below.

"It worth noting that the outer most parts of the outlet glaciers still have reasonable coverage and for studying changes in fast flow in these areas the increased temporal resolution may outweigh the downsides."
->
"For studies concerned with changes in fast flow in these areas the increased temporal resolution may outweigh the downsides."

Page 21, line 22: 'the increased temporal resolution may outweigh the downsides' – have you looked at a product using all 6 and 12 day pairs, but only over 1 cycle/12 days? I guess it will have reduced coverage and perhaps be less smooth, but may be useful for investigating the outlet glaciers.

The 6dOnly_1cycle is the product you are suggesting. It takes 12 days to cover all Greenland twice with a temporal baseline of 6 days, so there are no 12 day pairs that can be included. Figures 9 and 10 and Table 5 show that this product has lower coverage and is more noisy than the 2 S1A-cycle products due to the shorter temporal baseline of the included pairs, the S1A-B geolocation bias and simply because it contains fewer pairs. As you mention, the higher temporal resolution could easily outweigh these 'downsides' in cases, where the user is interested in the fastest flowing parts of the ice sheet. For that reason, the 6dOnly_1cycle may very well be a future product within PROMICE.

Page 24, line 5: This is the first mention of the extra log following the winter campaigns. I wonder if it would be better mentioned earlier?

Agree, we have included a sentence in the Section 'The PROMICE velocity product':
'However, during the winter campaigns where more data is acquired this lag may be larger.'

Page 24, line 18: 'vary' should be 'varies'
Done

Page 24, line 20: I suggest adding ', which hinder velocity retrieval' or similar after 'high precipitation rates'
Done

Page 24, line 25: add 'here' after 'presented'?

Done

Next, I list some minor spelling and/or grammatical errors and suggestions:

✓Page 1, line 2: comma before ‘which’

✓Page 1, line 4:’span’ should be ‘spans’

✓ Page 1, line 6: I think ‘6 and 12 day’ should be ‘6- and 12-day’ (here and throughout)

✓ Page 1, line 18: ‘Greenland Ice Sheet’ should be GrIS

✓Page 2, line 10: ‘SAR’ should be defined on first use.

✓Page 2, line 25: ‘Greenland wide’ should be ‘Greenland-wide’

✓Page 2, line 25: ‘IPP’ should be defined on first use.

✓Page 2, line 30: There should be a space after ‘i.e.’

✓Page 3, line 3: ‘timeseries’ is sometimes given as ‘time series’. I’m not actually sure which is correct, but I think you should be consistent.
We will use ‘time series’.

✓Page 3, last line: should ‘Wideswath’ be ‘Wide (IW) swath’?

✓Page 4, line 10: ‘5’ should be ‘Section 5’ (here and elsewhere)

Page 9, line 21: should that be four groups instead of ‘three’?

✓Page 10, line 8: I think ‘Southwest’ should be lowercase (there are similar errors throughout the manuscript).

✓Page 13, line 8: m/yr instead of m/s

✓Page 13, line 31: needs a comma after ‘Section 4.2’

✓Page 14, line 4: Does ‘Total Electron Content’ need to be uppercase?

✓Page 15, line 16: ‘(Boncori et al., 2018)’ should be ‘Boncori et al. (2018)’

✓Page 15, line 28: ‘can actually’ – should this be ‘could actually’? Or did you test this specifically?

✓Page 16, line 10: ‘in the top panel’, should instead just refer to the Figure/panel number/label. (same comment for line 15)

✓Page 17, line 14: ‘surface-properties’ doesn’t need to be hyphenated.

✓Page 17, line 20: need a comma after ‘baseline’

✓Page 20, first para: I found this a bit repetitive. I wondered if the penultimate sentence could be merged with the first sentence to streamline it a bit.

Agree. We have also inserted a missing data reference. The first paragraph in that section now reads:

‘We validate the PROMICE ice velocity product against in-situ GPS measurements. Only a limited number of GPS measurements are available since the data should overlap in time with the period of the PROMICE ice velocity product and have a a temporal resolution comparable to or higher than the PROMICE ice velocity product. Furthermore, the measurements are biased toward the slow moving 5 parts of the ice sheet ablation zone. We compare the PROMICE ice velocity product to in-situ GPS data from the PROMICE automatic weather stations (AWS) (van As et al., 2011). Locations are displayed in Fig. 11.’
->
‘We validate the PROMICE ice velocity product against in-situ GPS measurements from the PROMICE automatic weather stations (AWS) (van As et al., 2011; Fausto and van As, 2019) and perform an analysis over stable ground. Only a limited number of GPS measurements are available since the data must overlap in time with the period of the PROMICE ice velocity product and have a temporal resolution comparable to or higher than the PROMICE ice velocity product. Furthermore, the measurements are biased toward the slow moving parts of the ice sheet ablation zone. Locations are displayed in Fig. 12.’

✓Page 20, line 25: suggest adding ‘roughly’ before ‘east/west’

✓Page 21, line 12: is ‘Supp’ referring to the supplementary information in Hvidberg et al. (2019)? It’s not really clear whether it’s a typo.

No, we are also unsure how to cite the supplementary material correctly. We have changed the text to:
‘...values of 1.5 and 1.4 m/yr, respectively (supplementary material in Hvidberg et al., 2020). ‘

✓Page 21, line 21: ‘noticing’ should be ‘noting’? -> this sentence has been changed and no longer includes ‘noting’..

✓Page 21, line 32: ‘spatially better’ sounds a bit odd to me. Perhaps ‘A validation dataset that is not biased…’ would suffice? And/or mention that a spatial distribution representative of a greater range of observed ice velocities/flow regimes would help?

Agree, the sentence now reads:

A spatially better distributed set of validation data, which is not biased towards slow flowing areas in the ablation zone would help assess whether the reported product errors capture this correctly.
->

A validation dataset which is not biased towards slow flowing areas in the ablation zone but is representative of a larger range of flow regimes and surface conditions would help assess whether the reported product errors capture this correctly.

Below, I provide some feedback on the figures and figure captions

Figure 2: Are you sure the blue polygons represent radar image footprints? Some of them seem too large. Looking online, it looks like they might be acquisition segments instead? (Though I couldn't find a clear explanation of the difference). Can you also provide the dates for the 12-day periods shown?

The polygons represent the full segments acquired by the radar over Greenland, for each track. For practical reasons, these are split by ESA and delivered as 250 km x 250 km slices, which are designed to be easily concatenated into longer image strips. As for the dates, Fig.2a represents the tracks which are observed on every cycle, whereas the coverage shown on Fig.2b is for a single orbital cycle of the winter campaign 2019-2020 (repeated over 4 cycles). We have changed the figure caption to:

"Typical Sentinel-1 coverage over Greenland for a single 12-day orbital cycle, (a) during the standard observation scenario, (b) during the dedicated winter campaign from December 2019 - February 2020. The blue polygons represent acquisitions from different tracks, acquired at different times during the cycle."

Figure 3: Should the culling prior to mosaicking be included in the flow chart?

The flowchart has been updated to include details on the offset-tracking, including the culling prior to mosaicking.

Figure 4, caption: I don't think 'North' should be capitalised.

Figure 5, caption: Needs a space after 'a)'

Yes, a space has been inserted.

Figure 6: axis labels should have Va and Vr as Va and Vr

Fixed

Figure 7, caption: 'Pair' should be lower case.

Fixed

Figure 8, caption: '7' should be 'Figure 7'. 'Pair' should be lower case in both instances.

Fixed

Figure 9: Panels should be labelled a/b. I'm not sure the panel titles add much here either. The legend in the bottom panel blocks some of the data – can the scale of the yaxis be changed so that it doesn't block the lines, or can it be placed outside the graph?

Yes, the panels are now correctly labelled and the legend in the lower panel has been shifted, so it doesn't block the data. We have expanded the figure captions to include a better description of the figure.

Figure 10: I wondered if you could calculate the number of days in an average/given year for which there is velocity data in each pixel? That seems more intuitive to me than the current unit on the colour bar. Using something like that might also make it easier to refer to the values in the text. I think it would also be helpful to label the areas mentioned in the text.

What we aim to show with Figure 10 is where the user can expect good temporal data coverage throughout the time series and how it changes if not all possible pairs are included or if temporal resolution is increased. The temporal coverage depends on: * The number of acquisitions covering the grid point, which again depends on the time of year, the location and the time span of the product (the PROMICE product includes more pairs than any of the three other time series) *How often coherence is lost/ how often the processing fails. I am not sure how to calculate the number of days where there is coverage in a good way, and the figure in its current form shows the issues we want to highlight.
We have labelled Figure 10 a) so it shows the locations discussed in the text.

Accounting for the issues discussed above, we have changed the caption so it better describes the figure:

'Effect of including 6- and 12-day pairs on coverage in the mosaic: a) The PROMICE ice velocity product b) 6dOnly time series c) 12dOnly time series and d) 6dOnly_1cycle time series'
->
'Temporal coverage: Spatial view of the percentage of all mosaics in that have data in a given grid point: a) The PROMICE ice velocity product b) 6dOnly time series c) 12dOnly time series and d) 6dOnly_1cycle time series. The numbers in a) indicate the locations of the areas mentioned in Sec. 6: Areas where SAR in IW mode has not been acquired on a regular basis: 1, 2 and 3 refer to the triangular area in Melville Bay, North Greenland and the Scoresbysund area, respectively. Areas with low ice velocity coverage: 4, 5, 6 and 7 refer to the southeast ice sheet margin, small area in South Greenland, an area north of Rink Glacier and the Melville Bay area, respectively.'

We have changed the wording of the paragraph starting on P 17 L1:

'Figure 10 provides a spatial view of the fraction of all mosaics that have data in each grid point for each of the time series. Blue colors indicate that a grid point rarely has data, while yellow indicates a temporal coverage close to 100%. All four time series have a large blue area in the ice sheet interior, where SAR data in IW mode is rarely acquired as is evident from Fig. 2. The same explanation is true for the smaller triangular areas in the Melville Bay area and northern Greenland as well as the Scoresbysund area. However, the large blue/green area along the southeast ice sheet margin as well as an area in southern Greenland, one north of Rink Glacier inWest Greenland, and one in the Melville Bay area all have routine SAR IW acquisitions every 6 days. This will be discussed in the following.'
->

Figure 10 provides a spatial view of the temporal coverage of the time series. It shows the percentage of all mosaics that have data in a given grid point for each of the time series. Blue colors indicate that a grid point rarely has data, while yellow indicates a temporal coverage close to 100% . A number of circumstances influence the temporal coverage: The more acquisitions cover a grid point, the more likely it is to have a pair where coherence is not lost. The number of acquisitions depends on the time of year, the location and the time span of the product (the PROMICE product includes more pairs than any of the three other time series) The temporal coverage also depends on how often coherence is lost leading to how often the processing fails.

All four time series have a large low-coverage area in the ice-sheet interior, where SAR data in IW mode is rarely acquired as is evident from Fig. 2. The same explanation is true for the smaller triangular areas in the Melville Bay area and northern Greenland as well as the Scoresbysund area (locations 1, 2, and 3 in Fig. 11 a). However, the large area with low coverage along the southeast ice sheet margin as well as an area in southern Greenland, one north of Rink Glacier in West Greenland, and one in the Melville Bay area all have routine SAR IW acquisitions every 6 days (locations 4, 5, 6, and 7 in Fig. 11 a). This will be discussed in the following.

Figure 12: Inconsistent use of 'IV' and 'ice velocity' in the caption. Axis label font is a bit small. Rather than title the panels, I think labelling them a-c and describing them in the figure caption would be clearer. Axis labels should also be consistent with previous plots and text (i.e. use vx and vy).

'IV'' has been changed to ice velocity both in the caption but also in the figure labels. We have changed the titles of the subplots to better describe what the figure shows, and the subfigures has been labelled a, b and c.The figure caption has also been improved and now reads:

'*Scatterplots of PROMICE GPS IV vs PROMICE ice velocity.*'
->
'*Scatterplots of PROMICE GPS ice velocity vs PROMICE ice velocity. a): Scatter plot of the magnitude of the velocity. b): Scatter plot of the vx-component. c): Scatter plot of the vy-component*'

Table 4, caption: 'info' should be 'information'.
Agree -done.

Reviewer 3

Review of Solgaard et al.
Greenland ice velocity maps from the PROMICE project

This manuscript describes in detail an ice velocity (IV) products derived within the framework of the Programme for Monitoring of the Greenland Ice Sheet (PROMICE). IV products generated span an observation period of 24 days, are provided every 12 days and posted about 10 days after the last acquisition in the observation period. They are provided at 500 m posting in Polar Stereographic projection. The authors describe the Sentinel-1 data and ancillary data sets used for product generation, detail the automated product generation process and provide a comprehensive error assessment.

General comment:

This is one of several projects generating IV products for the Greenland ice sheet. The authors mention a number of other products in the introduction. What would be interesting here is how PROMICE IV fits within this lot given that the products are assessed in detail with slow moving areas as well as compared against GPS measurements. The authors encourage feedback from the community, so some information for the community through an inter-comparison of products as part of the product assessment would be considered an asset. The comparison with sub-sets of the product is a good first step, but seems insufficient.
The manuscript lacks justification regarding some of the product parameter choices. These parameters seem to be data driven (as opposed to science driven), which is fine, but some more discussion of trade offs would be helpful. Section 6 addresses some of this, but it does not fully explain all decisions.

- What drives the 500 m grid? Is this a suitable choice for all glaciers is Greenland, and if not, what percentage of glaciers is affected?

The choice of 500 m is driven by the spatial resolution of the measurements. Unfortunately this is not fixed for offset-tracking methods and not known a priori, since it is partially data dependent.
A lower bound is provided by the measurement spacing, which is 40 x 10 pixels in slant-range and azimuth, corresponding to 150 x 150 meters on ground. This would be the case for a measurement window containing a radar point target. However, this is not very realistic for ice-sheets, since, when the measurements rely on features, they are typically distributed targets, such as crevasses with a similar orientation. The upper bound on spatial resolution is instead determined by the cross-correlation window size, which is 256 x 64 pixels, corresponding to 800 x 900 meters on ground. 500 m represents a compromise between the lower and upper bounds, tending towards the latter, which is more representative of the true spatial resolution, since we are tracking either distributed targets, close to the ice-sheet margin, or intensity speckle, on the ice-sheet interior.

In the abstract and section 2, we have changed *"spatial resolution"* to *"grid spacing"* and we have added the following to section 2:
"*The effective spatial resolution is on the order of 800-900 m, determined by the fixed size of the correlation windows used in the offset-tracking (see Sect.4.2). Thus, glaciers smaller than approximately 1 km across will not be fully resolved."*

The following has been added to section 4.2:
"At each grid point, surrounding image patches of 256×64 complex pixels (slant range×azimuth) are extracted in both SLCs.This patch size has been chosen to maximize the coverage over different flow regimes and coherence levels, and means that the product has an effective spatial resolution on the order of 800-900m.As shown in (Boncori et al., 2018), an adaptive window size approach similar to the one described in (Joughin, 2002) could provide for a locally finer spatial resolution when the data allows it, but this is currently not implemented in the IPP processor"

- Why the 24 day (two S1A cycles) observation period? What is gained by averaging more (or less) data, what is lost? The discussion on page 19 does not feel sufficient.

We have added a summarising paragraph at the end of Section 6 to make our choice clearer based on the pro and cons of analysis carried out in the section:

'*The analysis from this section shows, that it is possible to provide a Greenland-wide ice velocity product with a higher temporal resolution than the PROMICE product (the 6dOnly_1cycle product), but also that this comes with the price of reduced spatial coverage and higher uncertainty. Creating a product spanning more than two Sentinel-1A cycles will have opposite effects: a reduction in uncertainty, a (small) increase in spatial coverage and reduced temporal resolution. The two Sentinel-1A cycles choice for the PROMICE product is therefore a compromise between having reasonably high temporal resolution and good coverage and reducing noise. '*

Different types of products are appropriate for different purposes: some users require high temporal resolution while others need complete coverage and low uncertainty.

- What drives the 10 day lag? It should be said that product generation 10 days after the last acquisition is impressive, the question is: Would 11 or 15 days be sufficient, is there anything to be gained for this to be 9 days?

The 10 day lag is simply the time it takes to include the last acquisition in the processing, do post-processing and have a time-buffer. We also state in the manuscript, that the 10 day lag is an aim and that it may take longer (or shorter) before the product is available. Stating when users can expect the product to update as well as it being relatively close to the time of the last acquisition are the most important aspects of this. Having a lag of 15 days vs 9 day most likely matters less, but for monitoring ice discharge and dynamics a lag of several months is not sufficient.

- With Landsat-8 and Sentinel-2 openly available, why the focus on Sentinel-1 for the product? This is not meant as criticism but a request for justification of the choice.

We are interested in obtaining mosaics all year round, and for this SAR data is great. It is not limited by clouds or darkness as is optical data (from e.g. Sentinel-2 or Landsat). Of course, using SAR data has limitations and including optical based ice velocities would enhance the product especially during summer where surface melt is a problem for SAR based products.

Section 3: Precision orbits

The web site provided http://aux.sentinel1.eo.esa.int/POEORB/ is outdated as of early March 2021. ESA has switched to another site (tbc) for the new orbits. Information for the products you refer to are still on the old site (as per review submission). Please provide the new site information as well.

The old website is no longer available - we have provided instead the new link: https://scihub.copernicus.eu/gnss/

Section 4.5: Culling

The existing time series data set is used to provide an average velocity to drive the culling of outliers. Seasonal variation of the ice speed is mentioned as an issue as it can exceed 200%. Would a seasonally limited average make a difference here, given that 4 years of data are already available?

It will certainly be worthwhile to improve the post-processing culling procedure in the future, and it is something we are working on. Seasonality would be a way to go, but the method would also have to not remove signals stemming from surge dynamics and longer term slow down or speed up. The culling method presented here is conservative, and not all outliers will be removed.

Section 5: Error

While not a big issue in Greenland, floating tongues have a tidal driven vertical displacement component that will be interpreted as speed if not corrected. At the very lest, this should be accounted for in the error

This is important to emphasize. We have added a sub-section (5.5) on tidal motion errors with the following text:

"*A few outlet glaciers in Greenland (Petermann and 79 Fjord being the most prominent) are characterized by having a floating tongue subject to tidal motion. The tidal motion introduces a vertical shift, with the sensitivity of this shift to the tidal signal increasing from 0 near the grounding line to 1 on the fully floating part of the tongue, a transition zone which is typically 5-10km wide (Padman et al., 2018). This vertical shift will affect the ice velocity estimate, as the difference in the shift between the two radar acquisitions is projected on to the radar line-of-sight and interpreted as motion in the slant range direction. In (Reeh et al., 2000), tidal-induced shifts of approximately +/-0.5 m were observed using GPS receivers placed on the floating part of 79 Fjord glacier. This could, for a 6-day pair, lead to errors in*

the ice velocity estimate of more than 50 m/yr, although the averaging of several acquisitions in the PROMICE product will tend to reduce this error. The effect is not modeled in the PROMICE product, so care should be taken when using the product on floating glaciers

Section 5.4: Ionosphere

The biggest impact of ionosphere perturbations are in azimuth direction. The available data are acquired in a way that for quite few regions you have ascending and descending data acquisitions available. Why not use the range - range components available in those regions to minimize the error?

We have adressed this in the answers to reviewer 1, which we repeat below:
The ionospheric effects are indeed the major error source, and we have experimented with methods relying on the dispersive properties of the ionosphere, similar to the ones described in (Gomba 2018) and (Liao et. al., 2018). However for Sentinel-1 TOPS data, there is a problem with block processing artifacts present in most Sentinel-1 SLCs, which severely hampers this approach. Another method to reduce the impact of ionospheric effects is to exploit the fact that in some regions, measurements from both ascending and descending tracks are available, and in this case one can derive the horizontal velocity from only the range offsets, which are much less affected by the ionosphere. This is being worked on, and will be included in a future update of the processor. We have added the following text:

"Another method to reduce the impact of ionospheric effects is to exploit the fact that in some regions, measurements from both ascending and descending tracks are available, and in this case, ice velocities can be derived from only the range offsets -- which are much less sensitive to ionospheric effects -- and the SPF assumption(see Sect.4.3). In the standard S1 acquisition plan (Fig. 2a), only two ascending tracks are acquired (the long track along the west coast of Greenland, and the track covering the northeast margin of the ice sheet up to the northernmost point), so the method will not be applicable everywhere. During the winter campaigns ((Fig. 2b), this method will be applicable in a much larger part of the ice sheet. Work is undergoing to include this method in a future update of the PROMICE product."

Section 7: Validation

The detailed validation against GPS measurements is appreciated.
Here, the evaluation of other existing Greenland IV products would have been a useful add On.

We agree that an evaluation of the various ice velocity products that are available is interesting, but we also find that this is out of scope for this data paper. In the paper, we validate our product against in-situ measurements, include an analysis over stable ground/ ice free areas as well as include the study by Hvidberg et al, 2020. All of which show that product performs well. We agree that it would be preferable to include in-situ measurements of fast flow, but we have not been able to find any. Comparison to other products would not solve this issue, since they have not been ground-truthed either at higher speeds.

Are the GPS data also available as a product? If so, please provide access information.

Yes, thank you. The data reference has been added.

Section 9: Summary and Outlook
Please provide the initial motivation for the product upfront

Page 24, lines 25,26:
" The PROMICE ice velocity product presented was originally intended primarily to calculate ice discharge through marine terminating glaciers of the GrIS as done in Mankoff et al. (2020)."

Yes, we already describe some of the uses of the product in the Introduction. We have expanded this sentence to:

"The product is used as input to, for example, the solid ice discharge product by Mankoff et al. (2020) and to study GrIS wide glacier dynamics in high temporal detail in Vijay et al. (2019)."
->
"The product is used as input to, for example, the solid ice discharge product by Mankoff et al. (2020) on a routine basis and to study GrIS wide glacier dynamics in high temporal detail in Vijay et al. (2019)."

Figures:
General comment: Sub-figures are not consistently named

Figure 2:
Based on the coverage maps the products have regionally different number of IV estimates and this number varies by season (with more Tracks covering the ice sheet during Winter). This is mentioned in Section 6 (page 19). Are the numbers for the estimates on a per pixel basis provided in the product somewhere? This seems relevant when comparing different maps.
This information is not provided in the PROMICE product, instead it is intended that the standard deviation maps be used for this purpose. Through the weighted averaging and standard deviation calculation, the fusion described in section 4.4 takes into account both the number of measurements and the quality of the measurements for each pixel. We believe this information is easier for the end user to apply than the number of measurements at each pixel.

Figure 3:
With the observation period set to 24 days, the minimum and maximum pair numbers are known and could be reflected in the figure.
The figure is meant as a high-level overview of the processing, and the number of pairs is the total number of data pairs (on all tracks) processed for the two S1A cycles comprising the PROMICE product. It will therefore vary, e.g. N would be much higher during the winter campaign. The figure has been updated to include offset-tracking details.

Figure 4:

Figure 4 and the corresponding discussion on page 9 would benefit from an assessment how many data points are culled (vs. how many outliers are not culled) for the various parameter selections.

Agree. We have included this information on P9 L10:

"For k_{thr}=3, the (real) summer speed up near the front is conserved, while the majority of spikes further inland are removed. Applying a stricter value, k_{thr}=1 removes not only outliers but also the real signal due to summer speed-up."

->

"For k_{thr}=3, the (real) summer speed up near the front is conserved, while the majority of spikes further inland are removed. Applying a stricter value, k_{thr}=1 removes not only outliers but also the real signal due to summer speed-up. In this case, 8 % of the pixels are culled while 4 % of the pixels are culled when applying k_{thr}=3."

Figure 5:

Figure 5 would benefit from a couple of insets providing more spatial detail of the culling.

We have expanded the figure to include zoom-ins of areas in western and eastern Greenland.

Fitures7, 8:

Figures 7 and 8 would benefit from being placed on the same page (or they should be combined to a single figure)

The figures have been placed together.

/ Figure 9:

Figure 9 has sub plots, should they not be a) and b)? Also, sub-figure annotation is inconsistent between figures.

Yes, a and b have been added to the subplots.

Product coverage is shown in multiple figures (1,2,5,(7,8),9,10), most of which provide spatial information. There is no such spatial information for the errors characterized by the STD shown in Figure 9. It would be useful to add the errors to one of the figures showing example maps (maybe Fig 1).

We have added a figure at the end of Section 5.5 Error Estimation showing the error estimate for the same mosaics we show in Figure 1. We have added a line of text at the end of the paragraph starting P15 L12:

'A Greenland-wide view of the error estimate for the PROMICE product is given in Fig. 8 for the same mosaics displayed in Fig. 9.'

Figure 9 product coverage indicates that culling is depending on the season. This

seasonality is of interest and could be shown in more detail.The authors use the STD as a proxy to estimate the error of the product. Does this hold in
the presence of strong ionospheric perturbations? In such cases the worst streaks are
culled but still have large area offsets causing a higher error in the product.

More points are culled in summer than in winter. We have added a time series to Figure 9 showing the percentage of points that are culled for each mosaic. Regarding ionopsheric perturbations, the impact of these are not fully reflected in the standard deviation estimate, due to the spatial correlation. We believe this is already described in Section 5.6 (Error estimates):
"The error estimates provided with the PROMICE ice velocity product are derived from the local standard deviation of the underlying shift maps generated by the offset-tracking (see Sect. 4.2 and 4.4). As such, they do not account for slowly varying errors, such as those described in Sect. 5.1 and 5.2, and only to a limited extent for the impact of ionospheric errors, as these are locally correlated on the scale of the window size used to estimate the local standard deviations."

Greenland ice velocity maps from the PROMICE project

Anne Solgaard[1], Anders Kusk[2], John Peter Merryman Boncori[2], Jørgen Dall[2], Kenneth D. Mankoff[1], Andreas P. Ahlstrøm[1], Signe B. Andersen[1], Michele Citterio[1], Nanna B. Karlsson[1], Kristian K. Kjeldsen[1], Niels J. Korsgaard[1], Signe H. Larsen[1], and Robert S. Fausto[1]

[1]The Geological Survey of Denmark and Greenland, Østervoldgade 10, 1350 København K, Danmark
[2]Technical University of Denmark - National Space Institute, Ørsteds Plads 348, 2800 Kongens Lyngby, Denmark

Correspondence: Anne Solgaard (aso@geus.dk)

Abstract. We present the Programme for Monitoring of the Greenland Ice Sheet (PROMICE) ice velocity product (https://doi.org/10.22008/promice/data/sentinel1icevelocity/greenlandicesheet (Solgaard and Kusk, 2021)), which is a September 2016 through present time series of Greenland Ice Sheet ice velocity mosaics. The product is based on Sentinel-1 synthetic aperture radar data and has a 500 m ~~spatial resolution~~grid spacing. A new mosaic is available every 12 days and ~~span~~ spans two consecutive Sentinel-1 cycles (24 days). The product is made available within ∼10 days of the last acquisition and includes all possible ~~6 and 12 day~~ 6- and 12-day pairs within the two Sentinel-1A cycles. We describe our operational processing chain ~~in high detail~~ from data selection, mosaicking and error estimation to final outlier removal. The product is validated against in-situ GPS measurements. We find that the standard deviation of the difference between satellite and GPS derived velocities (and bias) is 20 m/yr (-3 m/yr) and 27 m/yr ~~for the v_x and v_y components~~ (-2 m/yr) for the components in the eastern and northern direction, respectively. Over stable ground the values are: 8 m/yr (0.1 m/yr) and 12 m/yr (-0.6 m/yr) in the eastern and northern direction, respectively. This is within the expected ~~bounds~~values, however, we expect that the GPS measurements carry a considerable part of this uncertainty. We investigate variations in coverage from both a temporal and spatial perspective. ~~Best~~ The best spatial coverage is achieved in winter due to ~~excellent data coverage~~ the comprehensive data coverage by Sentinel-1 and high coherence, while summer mosaics have the lowest coverage due to widespread melt. The southeast Greenland Ice Sheet margin, along with other areas of high accumulation and melt, often have gaps in the ice velocity mosaics. The spatial comprehensiveness and temporal consistency make the product ideal for ~~monitoring and~~ both monitoring and for studying ice-sheet wide and glacier specific ice discharge and dynamics of glaciers on seasonal scales.

1 Introduction

The Greenland Ice Sheet (GrIS) is a major contributor to sea-level rise, and approximately half of this contribution is due to ice dynamics ~~(Shepherd et al., 2019; Mankoff et al., 2020)~~(Shepherd et al., 2019). Thus, in order to constrain the on-going mass loss of the ~~Greenland Ice Sheet~~ GrIS it is important to obtain ice-sheet wide observations of ice-flow velocities. High temporal and spatial resolution will further allow us to distinguish between annual or sub-annual variations and long-term trends, aiding in improving our understanding of the processes behind the observed changes. This is especially important because the flow of glaciers and ice caps vary on a range of timescales in response to the seasonal cycles, climate change, or internal variability

(e.g. Moon et al., 2020; Joughin et al., 2018; Mouginot et al., 2018). In-situ measurements of ice-flow velocities (e.g. from GPS) are relatively sparse on the GrIS and ~~most of the measurements stem from GPS surveys (Ahlstrøm et al., 2013)~~are often of short duration (months) at high temporal resolution (e.g. Sole et al., 2011; Maier et al., 2019) or of longer duration (years) but at low temporal resolution (e.g. Thomas et al., 1998; Hvidberg et al., 2020) while few span several years at high temporal resolution (e.g. Ahlstrøm et al., 2013). The sparseness is due to the inaccessibility and size of the GrIS and the harsh climatic conditions, which make fieldwork and instrumentation challenging. Satellite observations are thus key for deriving time series of ice velocity maps, which can increase our understanding of the dynamics of ice and its interactions with the other components of the climate system.

In the past, surface ice-velocity ~~(IV)~~ maps of the ~~Greenland Ice Sheet~~ GrIS and its outlet glaciers only resolved annual or seasonal characteristics due to the limited availability of data (e.g. Rignot and Kanagaratnam, 2006; Howat et al., 2010; Moon et al., 2014; Joughin et al., 2010)). This scenario changed with the launch of Landsat 8 (a joint NASA/USGS mission) in 2013, and ESA's Sentinel-1 (2014 and 2016) and Sentinel-2 (2015 and 2017) satellites. With this, freely available data became abundant, especially increasing the temporal resolution and spatial coverage of ice-velocity products. At present, several freely available GrIS wide velocity products exist with different temporal resolution e.g. annual, quarterly and monthly mosaics from Copernicus Climate Change Service, ESA-CCI (Nagler et al., 2015) and NASA's MEaSUREs program (e.g. Joughin, 2020a, c, b) including the ITS_LIVE project (Gardner et al., 2019) based on ~~SAR~~ synthetic aperture radar (SAR) and/or optical data. These are updated periodically with a lag. Scene pair velocities over Greenland from Landsat are available from NASA MEaSUREs ITS_LIVE at present up until 2018 (Gardner et al., 2019) and from TU Dresden covering the period (1972–2015) (Rosenau et al., 2015). Furthermore, Mouginot et al. (2019a, b, c, d) provide a freely available product comprising annual ice velocity mosaics for the GrIS spanning the period 1972 to 2017 based on both optical and SAR data.

Here we present the Programme for the Monitoring of the Greenland Ice Sheet (PROMICE) (www.promice.org) ice velocity product, which is a time series of ice velocity mosaics based on Sentinel-1 SAR offset-tracking. This work is part of the PROMICE monitoring effort focusing on the GrIS. The product benefits from the abundance, continuity, and high temporal resolution of the Sentinel-1 SAR data, and is continuously updated every 12 days. The product is used as input to, for example, the solid ice discharge product by Mankoff et al. (2020) on a routine basis and to study GrIS wide glacier dynamics in high temporal detail in Vijay et al. (2019). In the following sections we describe the ~~IV~~ ice velocity product, the data it is derived from, the operational setup, and the data processing steps that are used to generate it. Finally, we make use of available GPS measurements in order to validate our velocity product.

2 The PROMICE ice velocity Product

The PROMICE ice velocity product (https://doi.org/10.22008/promice/data/sentinel1icevelocity/greenlandicesheet (Solgaard and Kusk, 2021)) is a geospatial time series of ~~Greenland wide~~ Greenland-wide ice velocity mosaics produced using the IPP processor (see ~~Section~~ Sect.4). The product spans the period September 13 2016 to present and has a ~~spatial resolution~~ grid spacing of 500 m and a temporal resolution of 24 days.The effective spatial resolution is on the order of 800-900 m,

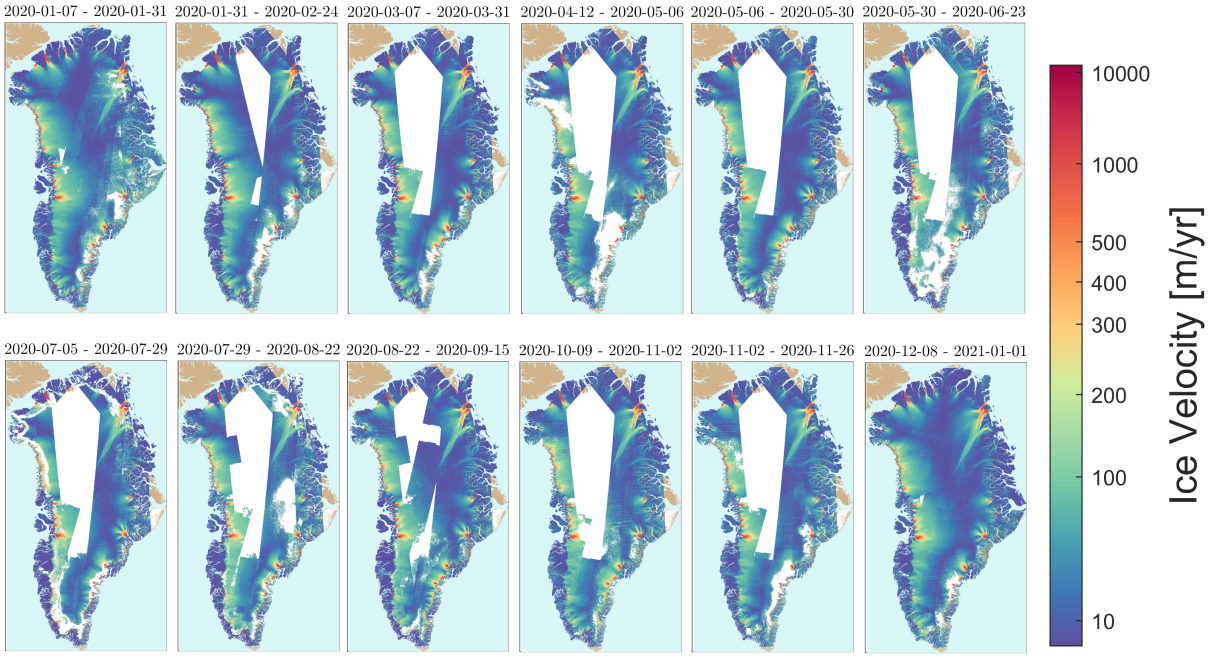

Figure 1. Examples of the PROMICE ice velocity maps from 2020: From top left corner to lower right approximately one map per month over 2020.

determined by the fixed size of the correlation windows used in the offset-tracking (see Sect. 4.2). Thus, glaciers smaller than approximately 1 km across will not be fully resolved. The product is based on measurements of displacements between pairs of radar images acquired 6 or 12 days apart (see ~~Section~~Sect. 3.1). To achieve a consistent coverage (see ~~Section~~Sect. 6), each mosaic is ~~a weighted average of~~ based on velocity measurements from all possible ~~6 and 12 day~~ 6- and 12-day pairs using data from Sentinel-1A and 1B within two consecutive Sentinel-1A orbit cycles (i.e.~~24~~ . 24 days). A ~~given mosaic thus overlaps by 12 days with the previous and subsequent maps. A~~ new map is produced for every Sentinel-1A cycle i.e. a new mosaic every 12 days. ~~We~~ A given mosaic thus overlaps by 12 days with the previous and subsequent maps. The dataset is expanded continuously, and we aim to provide a new mosaic within 10 days of the last acquisition. However, during the winter campaigns where more data is acquired this lag may be larger. The velocity provided at every grid point in the PROMICE ice velocity product is the weighted average of all velocity measurements available at that grid point within that 24-day period (see ~~Section~~ Sect. 4.4), and should be considered an average estimate of velocity over the 24-day period during which the radar images were acquired (see further discussion in ~~Section~~Sect. 6). The start and end times of this period are given in the *time_bnds* variable in the PROMICE NetCDF product (see below). Figure 1 shows samples of the ~~timeseries~~ time series at different times during the year ~~.~~ 2020.

Each ~~IV~~ ice velocity mosaic is supplied as a single NetCDF file following the Climate Forecast (CF) conventions (see https://cfconventions.org/). The mosaics are provided on a 500 m Polar Stereographic Greenland-wide grid with latitude of

Table 1. Variables in the PROMICE ice velocity NetCDF product

Variable	Description	Unit
x	x-coordinate of projection	m
y	y-coordinate of projection	m
time	Midpoint time of all contributing acquisitions	Days since 1990-1-1
time_bnds	First and last time of contributing acquisitions	Days since 1990-1-1
land_ice_surface_easting_velocity	Ice velocity along x-axis	m/d
land_ice_surface_northing_velocity	Ice velocity along y-axis	m/d
land_ice_surface_vertical_velocity	Vertical velocity from surface parallel flow	m/d
land_ice_surface_velocity_magnitude	Horizontal ice velocity magnitude	m/d
land_ice_surface_easting_velocity_std	Ice velocity error estimate along x-axis	m/d
land_ice_surface_northing_velocity_std	Ice velocity error estimate along y-axis	m/d
land_ice_surface_velocity_magnitude_std	Horizontal ice velocity error estimate	m/d

true scale at 70°N and reference longitude -45°E (EPSG 3413 projection). The variables in the NetCDF product are listed in Table 1. A quick look image for each mosaic is provided along with the dataset.

3 Data

In the following, we present the characteristics of the Sentinel-1 data and introduce the input data that we use to generate the PROMICE ice velocity product.

3.1 Sentinel-1 SAR Data Characteristics

SAR sensors are well suited for polar observations because data collection is not impacted by the polar night or cloud cover. The Sentinel-1 constellation currently consists of two satellites, Sentinel-1A and Sentinel-1B, equipped with identical C-band (5.4 GHz) SAR sensors. Over the GrIS, the Sentinel-1 SAR mainly employs the Interferometric ~~Wideswath~~ Wide Swath (IW) mode (De Zan and Guarnieri, 2006) allowing for generation of radar images with a resolution of approximately 3 m on ground in the slant range (line-of-sight direction) and 22 m in the azimuth (flight-path direction). The pixel spacing of the product is 2.3 m in slant range, and 14.1 m in azimuth.

The near-polar orbit has a repeat cycle of 175 orbits, corresponding to 12 days, with the two satellite orbits phased 6 days apart. With the current observation schedule, the entire margin of Greenland is imaged every 12 days by both satellites (Fig.~~2A~~ 2a). Furthermore, the entire ice sheet is mapped from several additional tracks every winter from December to February, allowing the generation of Greenland-wide maps during this season (Fig.~~2B~~ 2b).

SAR-based ice-velocity measurements are based on processing of image pairs. Images acquired within short time intervals (temporal baselines) retain a high degree of coherence (see ~~Section~~Sect. 5.3) and therefore measurement coverage, however

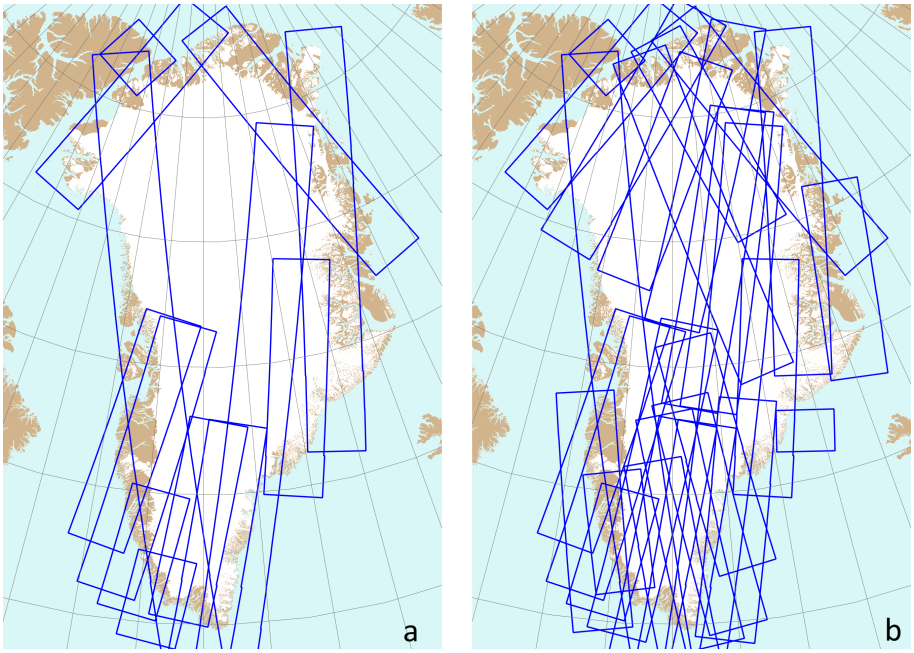

Figure 2. Typical Sentinel-1 coverage over Greenland for a single 12-day orbital cycle, ~~(~~a) during the ~~normal~~ standard observation scenario, ~~(~~b) during the dedicated winter campaign ~~.~~ from December 2019 - February 2020. The blue polygons represent ~~radar images~~ acquisitions from different tracks, acquired at different times during the cycle.

they also exhibit an increased sensitivity to error sources, which do not depend on the temporal baseline (e.g. processing artifacts, ionospheric and orbit estimation errors, see Sect. 5).

Image pairs can be formed between acquisitions from the same satellite, i.e. S1A-S1A or S1B-S1B, with temporal baselines which are a multiple of 12 days, i.e. 12-days, 24-days etc. In addition, image pairs can also be formed from acquisitions obtained from two different satellites, i.e. S1A-S1B or S1B-S1A, with a temporal baseline which is an odd multiple of 6-days, i.e. 6-days, 18-days, etc. Although in principle the radar instruments on board the Sentinel-1A and -1B satellites are identical, there are some subtle differences, which should be taken into account when selecting the data pairs for processing, as detailed in ~~sections~~ Sect. 4.1 and 5.2.

3.2 Input Data

The data used for generating the PROMICE ice velocity product are single-look complex (SLC) IW radar images (with annotation), supplied by the Copernicus Open Access Hub (https://scihub.copernicus.eu/). SLC images are focused SAR images referenced to the radar ~~acquisition~~ acquis ition geometry and have the highest resolution of the available IW product types (3 m $\times$ 22 m). They are supplied as slices with a footprint of approximately 250 km $\times$ 250 km. Owing to the peculiarities of the IW mode, each slice is subdivided into three range swaths, named IW1-IW3, which are acquired in an interleaved (bursted)

fashion; these swaths are stored in separate files. The SLC images are supplemented by restituted orbit files, available a few hours after acquisition, and precise orbit files, available 21 days after the data acquisition at https://scihub.copernicus.eu/gnss/. Since the PROMICE ice velocity product is typically generated before the latter become available, we use the restituted orbit files as we have found that the difference between the restituted orbit files and the precice orbit files is insignificant for our data products (see ~~Section~~Sect. 5.1).

In order to geocode measurements made in radar geometry, a digital elevation model (DEM) is used. We employ the ~~GIMP DEM (Howat et al., 2014)~~Greenland Ice Mapping Project (GIMP) DEM based on the ASTER and SPOT 5 DEMs and AVHRR photoclinometry (Howat et al., 2014, 2015), downsampled to 500 m spacing to match the resolution of the ~~IV~~ ice velocity product.

4 Methods

The data processing is carried out using the ~~IPP processor,~~ Interferometric Post Processing (IPP) processor, developed and maintained by DTU Space (Kusk et al., 2018). Despite the name, the processor also performs offset-tracking for displacement measurements, which is the functionality used to generate the PROMICE product. It is a highly automated processing chain requiring little user intervention. The ~~processor is developed and maintained by DTU Space (Kusk et al., 2018), and is~~ processing is described in the following ~~sections. An~~ section, and a high-level overview of the processing flow ~~can be seen~~ is shown in Fig. 3a.

4.1 Processing Flow

To support the PROMICE product generation, a database with all available SLC products over Greenland is maintained. This is updated daily by searching the Copernicus Open Access hub. An automated system downloads all new SLC data to a central storage location. Product generation is initiated by an operator selecting a Sentinel-1A reference orbit cycle number. All SLCs from Sentinel-1A in that and the following cycle (24 days of data) are first selected for processing. Additionally, all SLCs from Sentinel-1B acquired within the same 24-day timespan are selected for processing. Then, all possible SLC pairings with a 6- or 12-day baseline are calculated, and the offset-tracking processing described in Sect. 4.2 is automatically carried out for each pair. When all pairs required for a product have been processed, the geocoding and error estimation described in Sect. 4.3 and 5 is performed for each pair, followed by fusion and mosaicking of all the pairs, as described in Sect. 4.4.

4.2 Offset-tracking

The offset-tracking procedure employed is similar to the one described in Strozzi et al. (2002) and estimates local shifts between two SLCs in radar geometry ~~. First, the~~ using normalized cross-correlation of intensity image patches.It is illustrated in Fig. 3b.

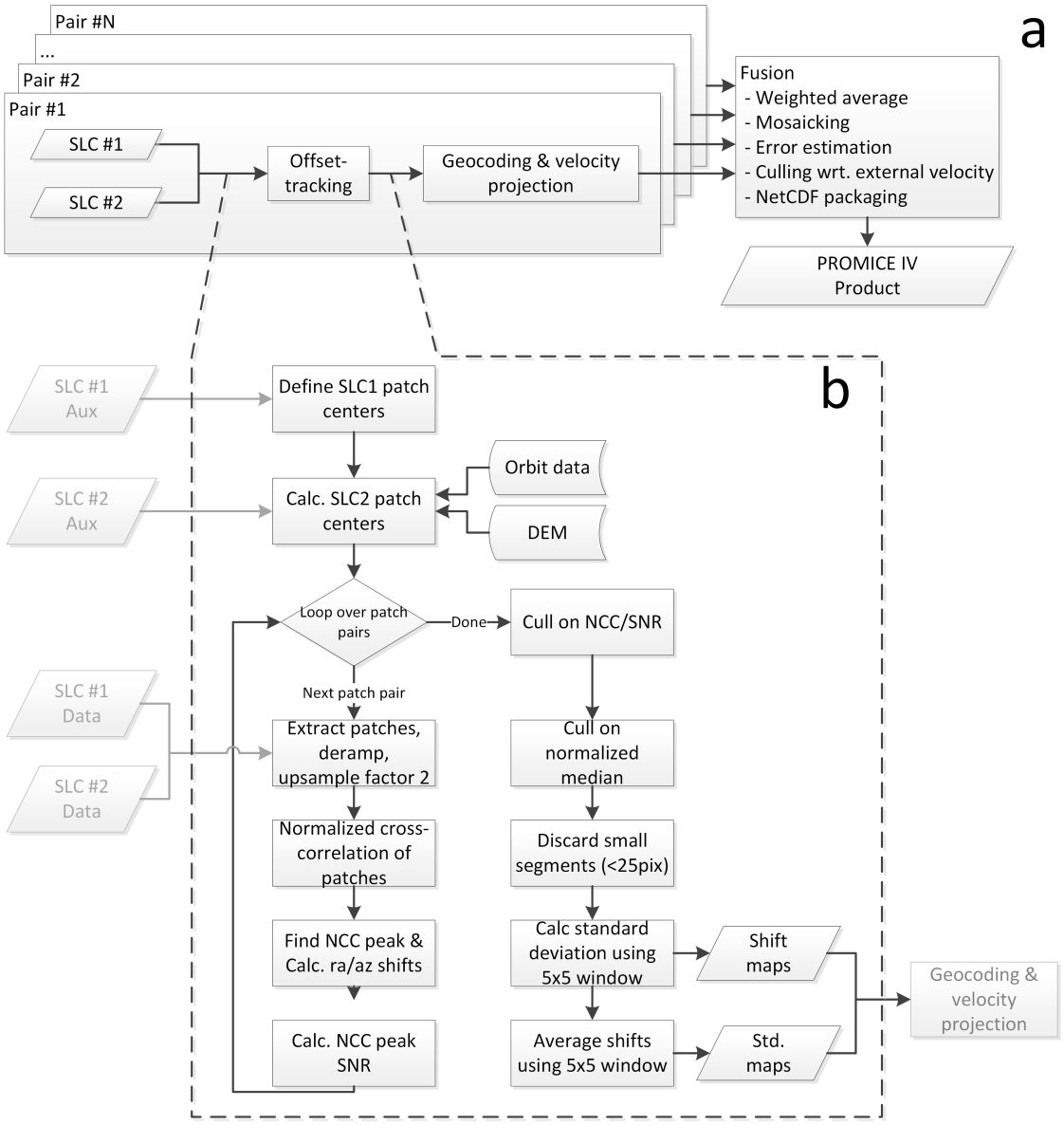

Figure 3. Processing flow for PROMICE ice velocity product~~generation~~, a) High level processing flow, b) Offset-tracking details.

The SLC with the earliest acquisition time is used as the reference image. Prior to the processing, calibration constants in range and azimuth timing are applied to correct for the different geolocation biases observed in Sentinel-1A and Sentinel-1B SLCs (see also Sect.5.2). For 12-day pairs, these constants are identical for both SLCs and have no effect.

An output grid is defined in the reference image geometry, with a spacing of 40 pixels in the slant-range direction and 10 pixels in the along-track (azimuth) direction. These spacings correspond to approximately 150 m×150 m on the ground. ~~The corresponding~~

For intensity cross-correlation methods, the SLCs need not be coregistered and resampled to sub-pixel accuracy prior to the processing, as they rely on relatively large windows (several tens of pixels in each dimension). Instead, for the regular grid points in the reference SLC, we calculate the expected position of the corresponding grid points (assuming no motion~~and including fractions of a pixel~~) in the second SLC~~are calculated using the SLC annotation, orbits~~, based solely on SLC timing information, orbital state vectors, and the DEM. ~~Calibration constants in range and azimuth are applied at this stage to correct for the different geolocation biases observed in Sentinel-1A and Sentinel-1B SLCs (see also 5.2). For 12-day pairs, these constants are identical for both SLCs and have no effect~~The grid points are selected on integer pixel positions in the reference SLC, but the corresponding grid points will generally not coincide with integer pixel locations in the second SLC. To avoid resampling the second SLC, we round the corresponding grid points to their nearest integer pixel locations and save the fractional shifts, which are then added back to the offset measurement after cross-correlation.

At each grid point, surrounding image patches of 256×64 complex pixels (slant range×azimuth) are extracted in both SLCs. ~~In the second SLC,~~ This patch size has been chosen to maximize the coverage over different flow regimes and coherence levels, and means that the product has an effective spatial resolution on the order of 800-900m. As shown in (Boncori et al., 2018), an adaptive window size approach similar to the ~~patches are extracted at integer pixel locations, with the fractional part saved to be added to the final shift estimate.~~ one described in (Joughin, 2002) could provide for a locally finer spatial resolution when the data allows it, but this is currently not implemented in the IPP processor Each patch is deramped (Miranda, 2017), upsampled by a factor of two (in both range and azimuth) using FFT interpolation, and the intensity (magnitude squared of the complex pixel values) is derived. A normalized cross-correlation of the two upsampled real-valued patches is carried out, resulting in a correlation surface with values between 0 and 1. The integer shift between the two patches is then estimated by locating the peak of the correlation surface, and a 9x9 neighbourhood surrounding the peak is upsampled by a factor of ~~4.~~ 4, again using FFT interpolation. Then the fractional shift is retrieved by fitting a parabola to the peak and its two surrounding pixels in each dimension, correcting finally for oversampling factors and accounting for the fractional shift initially estimated for the second SLC. A signal-to-noise ratio (SNR) for the peak estimate is calculated by dividing the correlation value of the peak with the mean of the surrounding pixels in the correlation surface (de Lange et al., 2007). The estimated 2-D shift, the peak normalized cross correlation value (NCC), and the SNR are all saved for further processing.

The procedure described above will yield a shift estimate even if the two images are completely uncorrelated, so a culling of the estimated shifts is carried out. First, pixels with an NCC<0.05 or SNR<7 are set as invalid. Then, a further culling, ~~based on local medians in~~ is carried out on the on the range and azimuth shifts, using a normalized median test, as described in (Westerweel and Scarano, 2005). For each measurement, U_0, in a 5×5 neighbourhood, ~~is carried out using the procedure described in Westerweel and Scarano (2005). These steps will remove most outliers, but some~~ the median, U_m, of the 24 surrounding measurements $(U_1, U_2, \ldots, U_{25})$ is calculated (excluding U_0), and for each measurement in the neighbourhood, a residual, $R_i = |U_i - U_m|$ is calculated. The median, R_m, of $(R_1, R_2, \ldots, R_{24})$ is then calculated, and used to normalize the

residual of U_0 so that $R'_0 = |U_0 - U_m|/(R_m + \epsilon)$, where ϵ is a minimum normalization level that accounts for cross-correlation noise. We use $\epsilon = 0.1$ pixel, as suggested in (Westerweel and Scarano, 2005), and cull the measurement,U_0, if R'_0 exceeds a threshold of 5 for either of the range or azimuth shifts. This value was found by experiments to remove most clearly visible outliers, without removing valid measurements. Lower values removed more outliers, but had an adverse effect on measurement coverage. After the culling, small unconnected segments of pixels (<25 pixels) are removed, as these were found to often contain erroneous values. Some outliers may remain, especially in areas subject to surface melt, as the associated strong radar backscatter can create false correlation peaks. An additional culling based on ~~timeseries~~ time series statistics (see ~~Section~~ Sect. 4.4) is carried out on the final mosaicked product to further suppress these outliers.

To aid in error estimation, the local standard deviations of the two shift maps (range and azimuth shifts) are estimated in a sliding 5×5 window, ignoring pixels with invalid measurements, and the shift maps are finally averaged by a 5×5 window. The shift maps (in units of SLC pixels) and associated standard deviations are stored along with the SLC parameters and orbit information to be used in the subsequent processing.

4.3 Geocoding and horizontal velocity projection

The geocoding takes as input the shift maps and associated standard deviation maps output by the offset-tracking and the DEM. Using the DEM and orbit information, the maps are ~~resampled~~ interpolated to the output grid in map projection (see ~~Section~~ Sect. 2). The shifts and standard deviations are converted to velocity by multiplying with the SLC pixel spacing and dividing by the temporal baseline. At this stage, the velocities and standard deviations, even though provided on a georeferenced grid, are still measured in the radar range/azimuth geometry. With a single pair providing only two velocity measurements, it is not directly possible to estimate three-dimensional flow. Instead, we assume surface parallel flow (SPF) and estimate the flow as described in the following. Let $\mathbf{v}_{xyz} = [v_x, v_y, v_z]^T$ be the three-dimensional velocity vector in map geometry, and $\mathbf{v}_{SAR} = [v_r, v_a]^T$ be the velocity vector in radar geometry, with v_r the range (line-of-sight) velocity and v_a the azimuth (along-track) velocity. With the SPF assumption, the vertical velocity component becomes (Joughin et al., 1998):

$$v_z = \left(\frac{\partial z}{\partial x} v_x + \frac{\partial z}{\partial y} v_y\right) \tag{1}$$

~~The partial derivatives can be~~ where $\left(\frac{\partial z}{\partial x}, \frac{\partial z}{\partial y}\right)$ is the surface gradient derived from the DEM~~, and the~~. The effective resolution of the velocity maps is on the order of the correlation window size, which corresponds to approximately 800 × 900 m on ground (see Sect. 4.2), so the resolution of the surface gradient map should approximately match this. The DEM is downsampled to the pixel spacing of the PROMICE product (500 × 500 m), and the gradient is derived using second order differences, which means the gradients are derived using samples approximately 1000 m apart. The relation between the horizontal and the radar velocity can be written as:

$$\begin{bmatrix} v_r \\ v_a \end{bmatrix} = \begin{bmatrix} \cos\theta\cos\phi + \sin\theta\frac{\partial z}{\partial x} & \cos\theta\sin\phi + \sin\theta\frac{\partial z}{\partial y} \\ -\sin\phi & \cos\phi \end{bmatrix} \begin{bmatrix} v_x \\ v_y \end{bmatrix} \tag{2}$$

where angles ϕ and θ describe the orientation of the line-of-sight (LoS) vector pointing from the pixel under consideration to the sensor, with the horizontal angle ϕ measured counter-clockwise from the y-axis of the map projection and the elevation

angle θ measured from the local horizontal plane to the LoS vector. The horizontal velocity components (and the associated standard deviation maps) can then be found by inversion of Eq. 2. Projection scaling factors are not applied to the velocities, so these represent physical velocities along the projection axes.

4.4 Fusion

The fusion step describes the process of combining and mosaicking the geocoded offset-tracking results on to a Greenland-wide grid. For every pixel on the output grid, we do a weighted averaging of the N valid velocity measurements from all pairs covering the pixel, using as weights the inverse of the measurement variances:

$$\hat{v} = \sum_{n=1}^{N} \frac{1}{\sigma_n^2} v_n \cdot (\sum_{n=1}^{N} \frac{1}{\sigma_n^2})^{-1} \tag{3}$$

where $\hat{v}$ is the fused (x or y) velocity, v_n is the (x or y) velocity measurement from pair n, and σ_n its associated standard deviation. The estimated standard deviation of the pixel is then:

$$\hat{\sigma} = \sqrt{(\sum_{n=1}^{N} \frac{1}{\sigma_n^2})^{-1}} \tag{4}$$

4.5 Culling

After all measurements have been fused and mosaicked, temporal culling is carried out to remove further outliers. This relies on comparison of the measured value with an average value of all available measurements, based at the time of writing on more than 4 years of data. For each pixel, we reject the measurement, if:

$$\frac{\sqrt{(\hat{v}_x - v_{m,x})^2 + (\hat{v}_y - v_{m,y})^2}}{\sqrt{v_{m,x}^2 + v_{m,y}^2} + v_\epsilon} > k_{thr} \tag{5}$$

where $(\hat{v}_x, \hat{v}_y)$ is the fused velocity measurement, $(v_{m,x}, v_{m,y})$ is the average velocity, v_ϵ is a velocity constant preventing erroneous culling in areas with very low velocities, and k_{thr} is a constant factor, setting the threshold for culling. A low value of k_{thr} will remove more outliers, but may also remove valid measurements in areas with strong seasonal variation, such as glaciers with significant speed up during the melt season. This effect is showcased for ice velocity along the flowline from Hagen Bræ in ~~North~~ north Greenland (Fig. 4a). The slow flowing outlet glacier ~~in North Greenland~~ experiences periods of speed up during summer, where velocities near the terminus increases more than 200%. At the same time surface melt inhibits processing parts of the data resulting in spikes in the ice velocity as evident in Fig. 4b. Figure 4c and d show how values of k_{thr}=3 and 1 cull the data. For k_{thr}=3, the (real) summer speed up near the front is conserved, while the majority of spikes further inland are removed. Applying a stricter value, k_{thr}=1 removes not only outliers but also the real signal due to summer speed-up. In this case, 8 % of the pixels are culled while 4 % of the pixels are culled when applying k_{thr}=3. For the PROMICE ice velocity product we apply, $v_\epsilon = 20$ m/yr, whereas $k_{thr} = 3$. This choice of threshold is a balance between removing as much noise as possible without removing actual signal in the mosaics encompassing a wide range of ice dynamics.

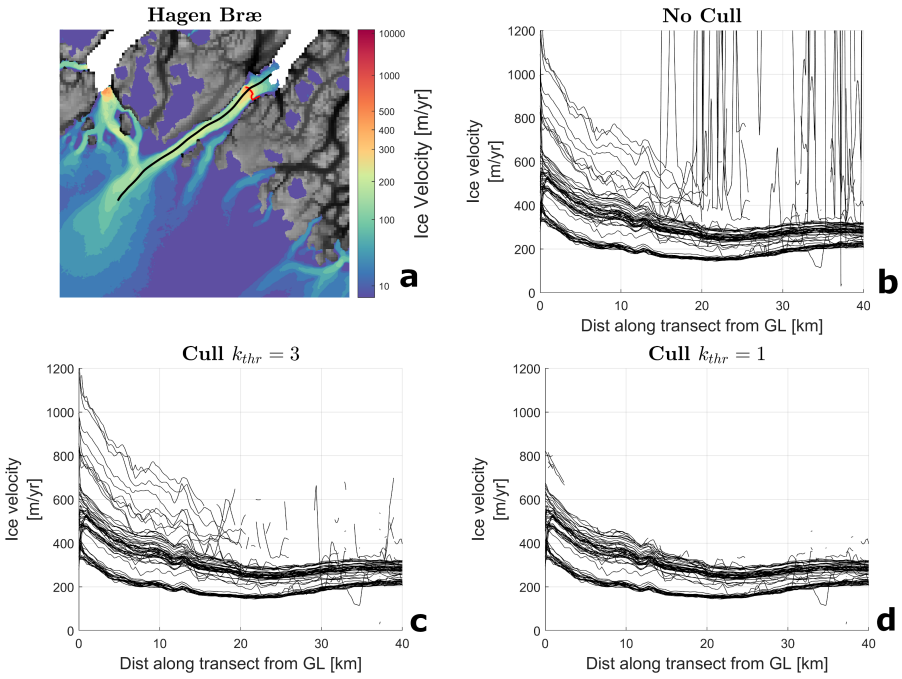

Figure 4. The effect of the culling procedure: Example from Hagen Bræ, ~~North~~ north Greenland. a) Overview of the Hagen Bræ area. The flowline is plotted in black and the grounding line (GL) (from ESA Greenland Ice Sheet CCI) is plotted in red. The ice velocity along the flowline in a) is plotted for all maps since September 2016 in the case of no culling b), applying k_{thr}=3 c) and applying k_{thr}=1 d).

Figure 5 provides an example of the effect of applying $k_{thr} = 3$ to a map from summer 2018 when surface melt influences the data quality. The unculled and culled maps are displayed in Fig. 5a and b. The location of the culled data points is shown in red in Fig. 5c. Note for example the removal of the noisy areas in the ~~West~~ west and east Greenland ablation zone ~~and~~ (Fig. 5c, d, and e) and locations influenced by ionospheric stripes in the slow moving interior. On average, ~ 2 % of the pixels in a mosaic are culled using this procedure. More pixels are culled in summer mosaics than in winter mosaics ~~.~~ (see Fig. 10a).

5 Error Sources and Estimation

In this section, we describe the error sources affecting the PROMICE ice velocity product in more detail. The error sources can be divided into three main groups:

1. Slowly varying errors, such as those caused by orbit errors (~~Section~~Sect. 5.1) or other timing biases in the products (~~Section~~Sect. 5.2).
2. Temporal decorrelation caused by changes in the radar backscatter between observations, see ~~Section~~Sect. 5.3.
3. Ionospheric errors, resulting in localized, but spatially correlated errors in the measured azimuth shift, see ~~Section~~Sect. 5.4.

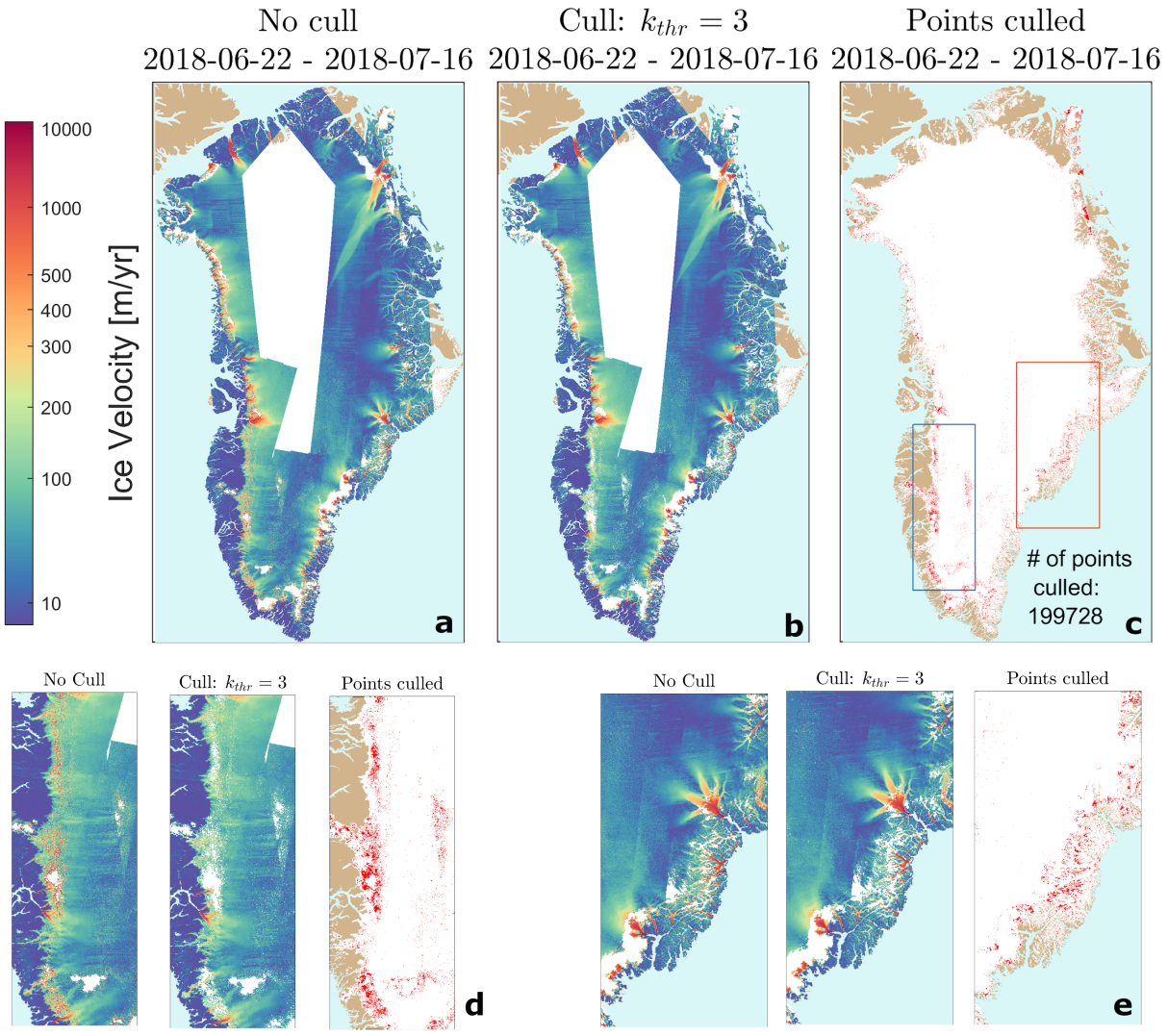

Figure 5. The effect of the culling procedure on the ~~Greenland Ice Sheet~~ GrIS scale for a map from summer 2018: a) The ice velocity map with no culling applied. b) The same ice velocity map with a culling threshold of k_{thr}=3 applied. c) The locations of the culled points are shown as red dots. d)Zoom-in on the blue box in western Greenland. e) Zoom-in on the red box in eastern Greenland.

4. Aliasing errors caused by the need to acquire two observations from which we infer displacement, and then velocity. Any extreme velocity highs or lows will be smoothed out.

5. Errors due to tidal motion of floating glacier tongues.

Table 2. Comparison of precise and restituted orbits files. Range direction is line of sight and azimuth direction is along the satellite flight path

Orbit Type	Range Velocity Bias [m/yr]	Range Velocity Std [m/yr]	Azimuth Velocity Bias [m/yr]	Azimuth Velocity Std [m/yr]
Precise	-0.5	2.7	0.4	3.3
Restituted	-0.5	2.8	0.4	3.3

5.1 Orbit Errors

Errors in the ~~knowledge of the~~ Sentinel-1 ~~satellite orbits~~ orbital state vectors provided by ESA will result in an apparent shift between the two SLCs in a pair, translating directly into biases on the velocity measurement. For Sentinel-1 data, absolute orbital errors are on the order of 5cm RMS when using the precise orbit product available after 21 days (Peter et al., 2017). The restituted orbits typically used in the PROMICE product generation are available shortly after acquisition, and have a nominal accuracy of 10 cm RMS. This corresponds to ~~3~~ 8.6 m/yr RMS for a measurement using a 6-day pair and ~~1.5~~ 4.3 m/yr for a 12-day pair. ~~Restituted orbits (which are available shortly after acquisition rather than 21 days later) have a nominal accuracy of 10 cm RMS.~~

To assess the difference between using restituted and precise orbits, we processed 18 different Sentinel-1 12-day pairs (9 S1A/S1A and 9 S1B/S1B pairs) acquired consecutively over an area in ~~Southwest~~ southwest Greenland where much of the scene in the IW1 swath consists of bedrock. The reason for using only 12-day pairs is to exclude the effect of S1A-S1B biases, which are treated instead in ~~Section~~ Sect. 5.2. All pairs were processed twice, using either the precise orbits or the restituted orbits, with all other parameters identical. The processing carried out consisted of offset-tracking and geocoding (see ~~sections~~ Sect. 4.2 and 4.3). Averaging for each processed pair the measured range and azimuth velocities over the bedrock area, which can be assumed stationary, gives an estimated average residual velocity error for that pair. The mean of the 18 residual range and azimuth velocity estimates and associated standard deviations are listed in Table 2. We note that the range velocity bias (-0.5 m/yr) and azimuth velocity bias (0.5 m/yr) do not differ between the precise and the restituted orbit files. The ~~range standard deviation~~ standard deviation in the range direction is 2.7 m/yr for the precise orbit files and 2.8 m/yr for the restituted orbit files, while the ~~azimuth standard deviation~~ standard deviation in the azimuth direction is 3.3 m/yr for both orbit types. Overall, the error statistics for the two orbit types are almost completely identical, and the use of restituted versus precise orbits has an insignificant impact on the accuracy of the final velocity products.

5.2 Geolocation Bias Correction

With the commissioning of Sentinel-1B in late 2016 it became possible to generate ice velocity products with a 6-day temporal baseline by combining Sentinel-1A and Sentinel-1B data (see also 3.2). Although the SAR instruments are in theory identical, our analysis of the initially generated 6-day ice velocity products revealed velocity biases not present in 12-day (same satellite)

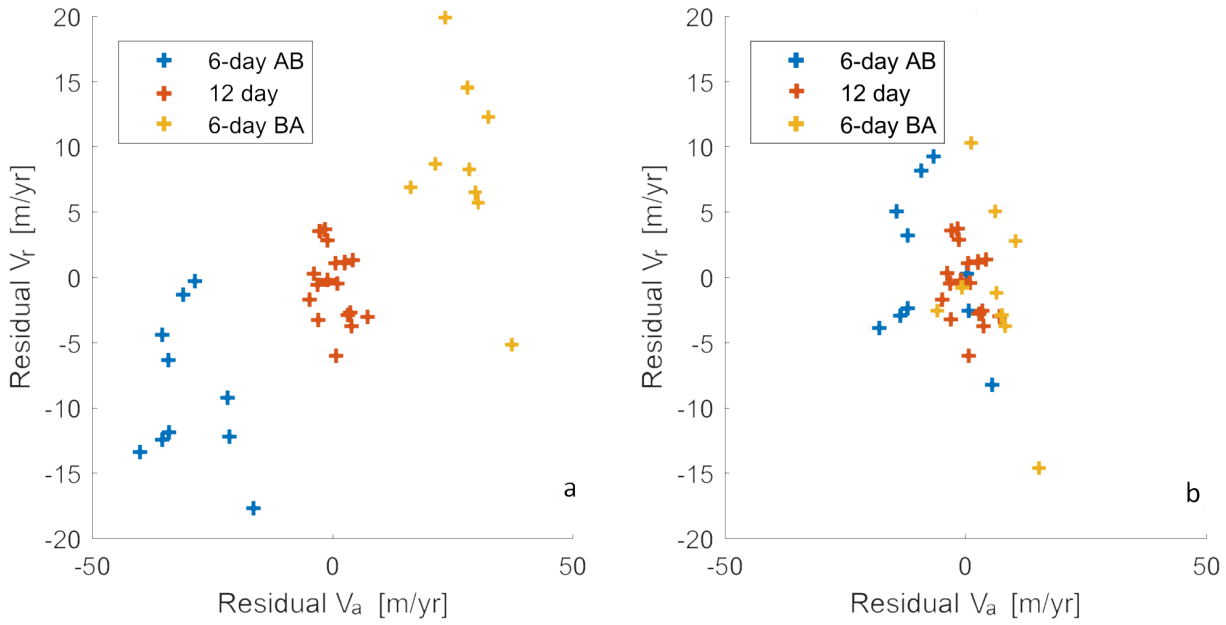

Figure 6. Scatterplot of IW1 average residual range (v_r) and azimuth (v_a) velocity error of 37 Sentinel-1 pairs, (a) without calibration, (b) calibrated with constants from (Gisinger et al., 2020).

Table 3. Velocity biases for different satellite combinations

Pair Type	Range Bias [m/yr]	Range Std [m/yr]	Azimuth Bias [m/yr]	Azimuth Std [m/yr]
12-day AA/BB	-0.5	2.7	0.4	3.3
Uncalibrated 6-day BA	-8.9	5.7	-29.9	7.6
Uncalibrated 6-day AB	8.6	6.9	27.5	6.3
Calibrated 6-day BA	0.6	5.7	-7.9	7.6
Calibrated 6-day AB	-0.9	6.9	5.5	6.3

pairs. To quantify this, an experiment was carried out using 37 Sentinel-1 pairs (9 6-day A/B pairs, 10 6-day B/A pairs, and 18 12-day A/A and B/B pairs grouped together). The 18 12-day pairs are identical to the pairs used in 5.1, thus, all pairs were acquired over an area in ~~Southwest~~ southwest Greenland where much of the scene in the IW1 swath consists of bedrock. Averaging the measured range and azimuth velocity over the bedrock area, gives an estimated average residual velocity error for that pair. Figure 6a shows a scatterplot of the residual range velocity (V_r) versus residual azimuth velocity (V_a) for the 37 pairs. The corresponding mean and standard deviation values are listed in Table 3.

As expected, the 12-day statistics are identical to those observed in the orbit type comparison (see Section 5.1 and Table 2), with a bias magnitude below 0.5 m/yr. For the 6-day pairs (middle part of Table 3), the bias magnitudes are significantly larger and change sign, depending on whether the first SLC in the pair is acquired from Sentinel-1A or Sentinel-1B. The standard deviations of the 6-day bias estimates are approximately two times those of the 12-day estimates, which is expected, as the velocity measurements are based on measurements of shifts between the images, which are then divided by the temporal baseline to arrive at velocities. The average bias magnitudes for the 6-day pairs are 8.8 m/yr in range and 28.8 m/yr in azimuth. With the 6-day baseline, this corresponds to bias magnitudes on the measured shifts of 0.15 m in range and 0.48 m in azimuth. These values are consistent with results obtained in detailed analysis of Sentinel-1 SLC product geolocation using corner reflectors, see (Schubert et al., 2017) and (Gisinger et al., 2020). The latter reports average shifts between Sentinel-1A and Sentinel-1B of 0.16 m in range and 0.40 m in azimuth, corresponding to velocities of 9.7 m/s yr and 24.4 m/syr, respectively, for measurements using 6-day pairs, but also suggests that there may be a swath dependence of these delaysshifts. Our analysis above concerns only the IW1 swath, so for now, we use the constants from (Gisinger et al., 2020) mentioned above to calibrate the PROMICE product. The calibration is implemented as an adjustment to the timing annotation for the SLC products prior to the offset-tracking. Applying these calibration constants to the test dataset described above results in a significantly reduced bias on the 6-day measurements, as shown on Fig. 6b and in the bottom part of Table 3. The calibrated 6-day range velocities now have a mean bias magnitude of 0.8 m/yr, and the azimuth velocities a mean bias of 6.7 m/yr. In the final PROMICE ice velocity product, the weighted averaging of 12-day pairs and both A/B and B/A 6-day pairs will tend to reduce the impact of any residual biases (see also 4.4).

5.3 Temporal Decorrelation

Temporal decorrelation is caused by changes in radar backscatter between acquisitions , affecting the ability to measure ice velocitythat reduce the correlation between the image patches which are cross-correlated in the offset-tracking procedure, leading to noisy or even missing measurements. The surface of the interior of the ice sheet is relatively homogeneous, with no large scale features, and the velocity measurement relies on preservation of the speckle pattern (coherence) between observations (Gray et al., 1998). Speckle is a property of radar images, caused by variations in the sub-resolution structure of the imaged scene, resulting in large pixel-to-pixel intensity fluctuations in otherwise homogeneous areas. If the scene is moving, but otherwise stable, ice-flow is spatially uniform and the sensor images the scene from the same tracktrack does not deviate excessively for the two acquistions (the latter is generally not a problem for Sentinel-1), the speckle pattern can be tracked between acquisitions using the cross-correlation procedure described in Section 4.2. Precipitation, surface melt, and rapid steep spatial gradients in ice flow can all reduce the coherence and thus the ability to measure ice velocity in such areas. Often in the interior, the noise level exceeds the signal, but signal-to-noise ratio is low, but since five velocity maps from each track are averaged to produce the PROMICE product, the measurements can still be useful, by averaging multiple measurements to reduce the noise noise can be reduced. In extended homogeneous areas of low coherence, the velocity measurements can become noisy and patchy, since many unreliable measurements will be discarded by the culling procedures described in SectionsSect. 4.2 and 4.5.

On outlet glaciers, the rapid ice flow and associated deformation tends to destroy the coherence except for short temporal baselines. Here, the ability to measure displacement relies instead on the presence of larger scale features, such as crevasses, which can be still be tracked between images with the cross-correlation procedure described in ~~Section 4.2~~Sect. 4.2, even if there is no coherence.

Models that express the shift errors as function of coherence do exist (De Zan, 2014), but the coherence cannot directly be used to estimate errors or discard measurements, since velocity measurements can often still be made in non-coherent, fast moving areas, as mentioned above. In the PROMICE ice velocity product, the velocity error estimate is based instead on the local standard deviation of the tracked shifts (see ~~Sections~~Sect. 4.2 and 5.6).

5.4 Ionospheric Errors

Ionospheric propagation errors arise due to spatial fluctuations (scintillations) in the ionosphere ~~Total Electron Content~~ total electron content within the SAR synthetic aperture length (i.e. km-scale variations) (Gray et al., 2000). This is especially a problem in the near-polar regions. For a given image pixel, these fluctuations cause an azimuth variation in the raw signal phase, which is not accounted for by the SAR focusing, resulting in an azimuth shift of the focused pixel. The varying propagation naturally also causes a shift in the range direction, but these shifts are much smaller (typically on the centimeter-level) than those observed in the azimuth direction (comparable to the azimuth pixel size, i.e. several meters (Mattar and Gray, 2002)). The shifts vary along the scene according to the ionosphere conditions along the satellite flight path, often present in only parts of the scene. Also the observed shifts are strongly correlated in the range direction, appearing as linear or slightly curved "streaks" superposed on the azimuth shift map. In the PROMICE velocity mosaics, such streaks are readily identifiable by the human eye, appearing as roughly ~~East-West~~ east-west oriented stripes of varying intensity. The velocity errors caused by ionosphere can exceed 200 m/yr, impacting 6-day pairs twice as much as 12-day pairs, since the shifts caused by the ionopshere do not depend on the temporal baseline. An example of the impact of the ionosphere can be seen in Fig. 7 showing a single-pair 6-day velocity measurement and a 12-day velocity measurement, the former exhibiting significant ionospheric streaks. Both pairs share a common SLC (acquired 2016-10-11), suggesting in this case that the ionosphere effects can be attributed to the other SLC of the 6-day pair.

Methods for reducing the impact of the ionosphere on ice velocity measurements typically rely on the dispersive nature of the ionosphere delay, and have been applied to L-band interferometric ice velocity measurements (Liao et al., 2018). A method for correcting azimuth shift measurements in Sentinel-1 data has been proposed in (Gomba, 2018), but has not been demonstrated for Sentinel-1 ice velocity measurements. Another method to reduce the impact of ionospheric effects is to exploit the fact that in some regions, measurements from both ascending and descending tracks are available, and in this case, ice velocities can be derived from only the range offsets — which are much less sensitive to ionospheric effects — and the SPF assumption (see Sect.4.3). In the standard S1 acquisition scenario (Fig. 2a), only two ascending tracks are acquired (the long track along the west coast of Greenland, and the track covering the northeast margin of the ice sheet up to the northernmost point), so the method is not always applicable everywhere. During the winter campaigns ((Fig. 2b), this method will be applicable over a much larger part of the icesheet. Work is undergoing to include this method in a future update of the PROMICE product.

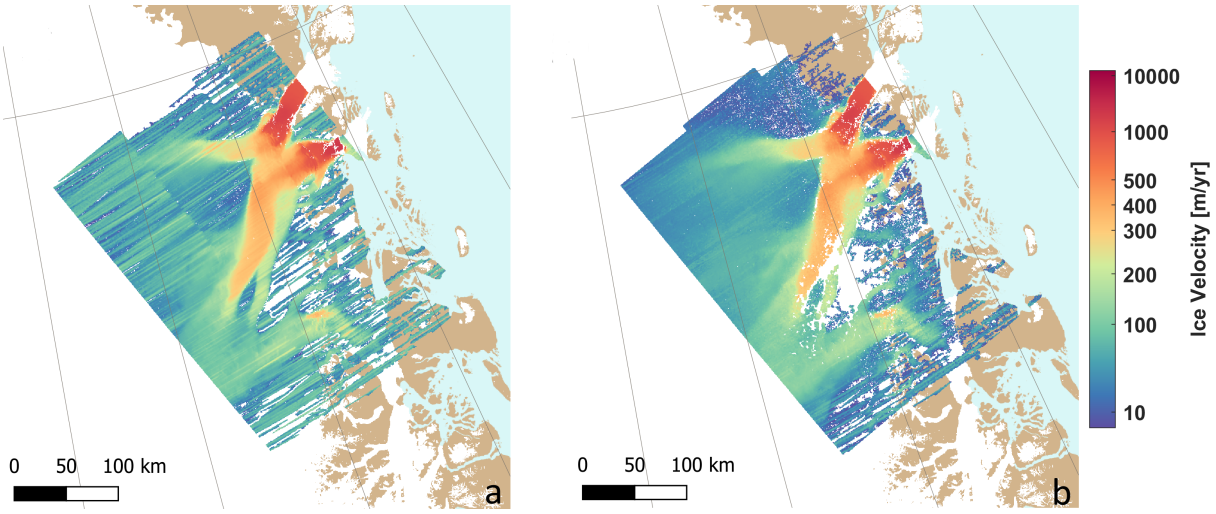

Figure 7. Two single-pair velocity maps from relative orbit 74 (ascending), illustrating the impact of ionospheric streaks, ~~(~~a) 6-day ~~Pair~~ pair acquired 2016-10-11 and 2016-10-17, with strong ionosphere errors, ~~(~~b) ~~Pair~~ 12-day pair acquired 2016-10-11 and 2016-10-23, with limited ionosphere errors.

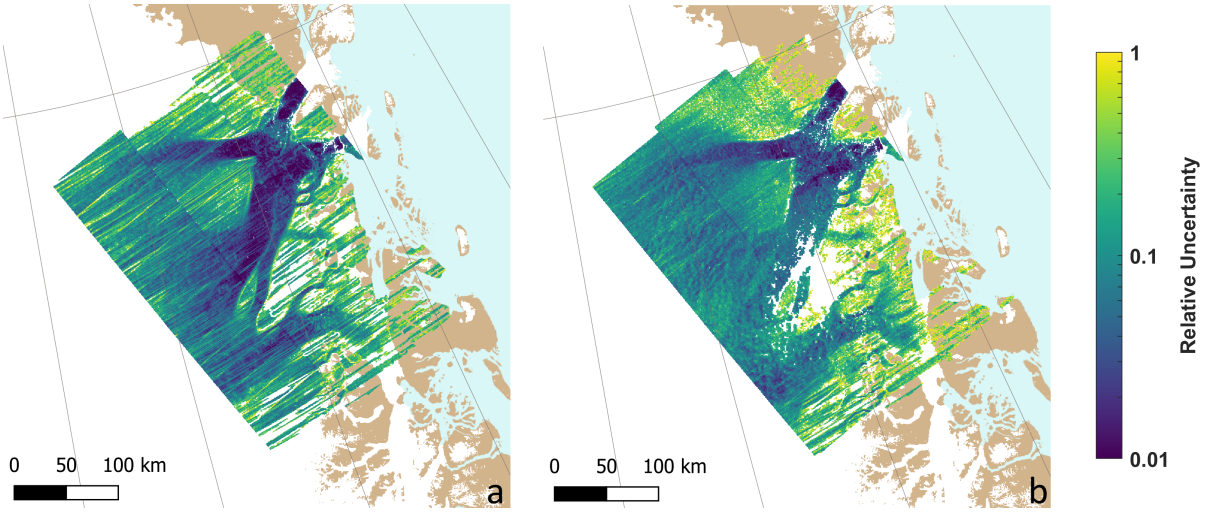

Figure 8. Relative horizontal velocity error estimates for the single-pair velocity maps in Fig. 7, a) 6-day pair acquired 2016-10-11 and 2016-10-17, b) 12-day pair acquired 2016-10-11 and 2016-10-23.

The mitigation of ionospheric effects in the PROMICE ice velocity product relies on culling and averaging. Pixels with large ionospheric errors, if present in regions with generally low velocities, will be removed by the temporal culling procedure described in Sect. 4.4. In areas where multiple velocity observations are available, the weighted averaging in the fusion (see Sect. 4.4) will tend to reduce, but not completely remove, the ionospheric effects. We estimate that the ionospheric effects can

cause a velocity error of up to 300 m/yr and will mainly affect the v_y-component, which is roughly aligned with the azimuth direction due to the near-polar orbit of the Sentinel-1 satellites.

5.5 Tidal motion

A few outlet glaciers in Greenland (Petermann and 79 Fjord being the most prominent) are characterized by having a floating tongue subject to tidal motion. The tidal motion introduces a vertical shift, with the sensitivity of this shift to the tidal signal increasing from 0 near the grounding line to 1 on the fully floating part of the tongue, a transition zone which is typically 5-10 km wide (Padman et al., 2018). This vertical shift will affect the ice velocity estimate, as the difference in the shift between the two radar acquisitions is projected on to the radar line-of-sight and interpreted as motion in the slant range direction. In (Reeh et al., 2000), tidal-induced shifts of approximately +/-0.5 m were observed using GPS receivers placed on the floating part of 79 Fjord glacier. This could, for a 6-day pair, lead to errors in the ice velocity estimate of more than 50 m/yr, although the averaging of several acquisitions in the PROMICE product will tend to reduce this error. The effect is not modeled in the PROMICE product, so care should be taken when using the product on floating glaciers.

5.6 Error Estimation

The error estimates provided with the PROMICE ice velocity product are derived from the local standard deviation of the underlying shift maps generated by the offset-tracking (see ~~Sections~~Sect. 4.2 and 4.4). As such, they do not account for slowly varying errors, such as those described in ~~Sections~~Sect. 5.1 and 5.2, and only to a limited extent for the impact of ionospheric errors, as these are locally correlated on the scale of the window size used to estimate the local standard deviations. Although this is not a complete error characterization, it was shown in ~~(Boncori et al., 2018)~~ Boncori et al. (2018) to provide the correct order of magnitude for the errors. Examples of relative error estimates accompanying the two ice velocity maps from Fig. 7 are shown in Fig. 8. The strong ionospheric streaks evident in the 6-day pair on Fig. 7 are seen to be reflected in the corresponding error estimate, although the magnitude is underestimated. In the central and lower left part of the maps, errors are seen to be generally higher on the 12-day pair, but in a more diffuse pattern, even though the 12-day pair is less sensitive to a given shift error, due to the longer baseline. In this case, it is the higher temporal decorrelation of the 12-day pair that causes an increased noise level, which is also reflected in the error estimate. A Greenland-wide view of the error estimate for the PROMICE product is given in Fig. 9 for the same mosaics displayed in Fig. 1.

~~Relative horizontal velocity error estimates for the single-pair velocity maps in 7, (a) 6-day Pair acquired 2016-10-11 and 2016-10-17, (b) 12-day Pair acquired 2016-10-11 and 2016-10-23.~~

The slowly varying errors (~~Sections~~ Sect. 5.1 and 5.2) could potentially be corrected by calibrating the measured velocities using ground control points (GCPs), either on stable terrain or in areas where the ice flow is known to vary little. In practice this is difficult to do in an automated system, as the calibration has to be carried out on the individual pairs, where the ionospheric and, to some extent, the temporal decorrelation errors associated with offset-tracking are often much larger than the slowly varying errors. If GCPs are unwittingly selected in areas affected by e.g. ionosphere, the GCP calibration ~~can~~ could actually have a detrimental impact. A large number of GCPs, well distributed in the image, would be required to reduce the statistical

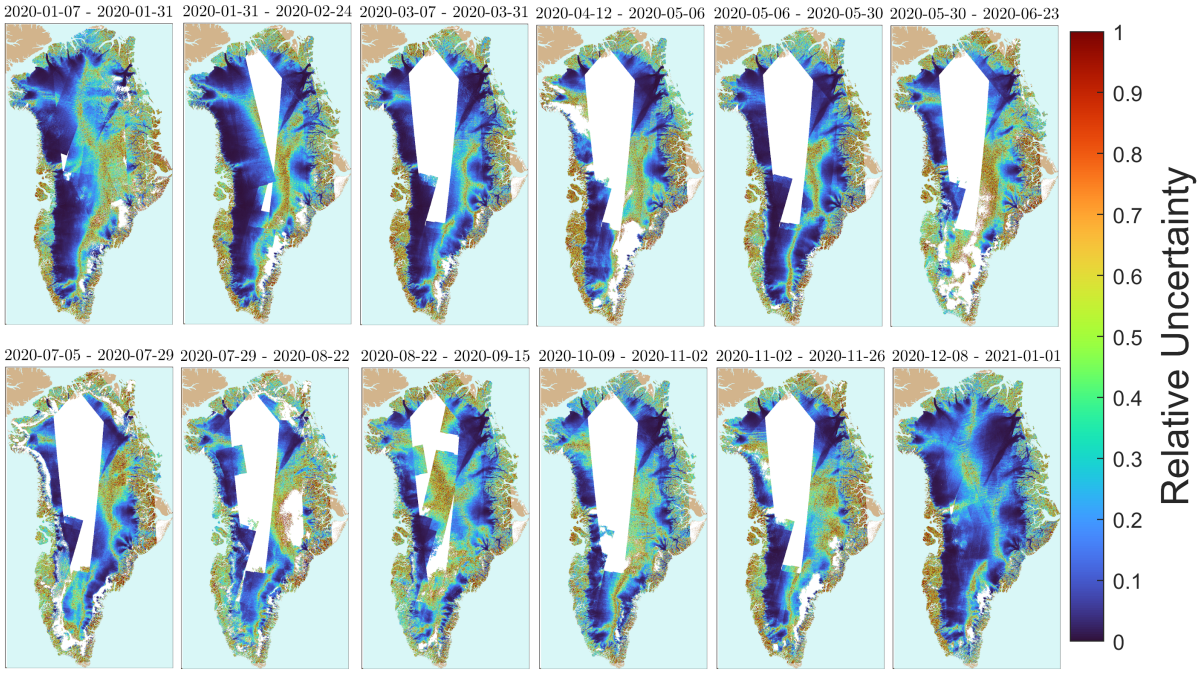

Figure 9. Greenland-wide view of the error estimates for the PROMICE mosaics displayed in Fig. 1.

noise, but this can often not be achieved within the limited spatial coverage of a single pair. For this reason, the PROMICE ice velocity product is not calibrated using GCPs.

6 Properties of the ~~Promice~~ PROMICE Ice Velocity Product

The PROMICE ice velocity product is designed as a compromise between good spatial coverage, high temporal resolution, and low noise. Other combinations of 6 day and 12 day pairs are possible resulting in ~~different a~~ a different temporal resolution and spatial coverage. We explore other possibilities for products and compare them to the PROMICE ice velocity product with respect to coverage and noise. These products are time series of mosaics consisting of (see Table 4):

1. All 6 day pairs (no 12 day pairs) within 2 Sentinel-1A cycles (**6dOnly**).
2. All 12 day pairs (no 6 day pairs) within 2 Sentinel-1A cycles (**12dOnly**).
3. All 6 day pairs (no 12 day pairs) within 1 Sentinel-1A cycle (**6dOnly_1cycle**).

Time series number 3, **6dOnly_1cycle**, thus has twice the frequency compared to the PROMICE product.

Data coverage for each mosaic in each time series is displayed in ~~the top panel of~~ Fig. 10a. We defined the coverage as the fraction of grid points that contains ice velocity data on the ice sheet in a given mosaic. We have included a time series in the

Table 4. ~~Info~~ Information on ~~timeseries~~ time series of mosaics from Sentinel-1 data. All-pairsNoCull contains the same data as the PROMICE product, but has not undergone the culling procedure described in ~~Section~~Sect. 4.5.

	Temporal resolution	All 12d pairs included	All 6d pairs included
PROMICE Product (All-pairs)	24d	x	x
6dOnly	24d		x
12dOnly	24d	x	
6dOnly_1cycle	12d		x
All-pairsNoCull	24d	x	x

analysis called **All-pairsNoCull**, which includes the same data as the PROMICE product, but has not undergone the culling procedure described in ~~Subsection~~Sect. 4.5.The percentage of points that are culled in each mosaic of the PROMICE product using that method is also shown in Fig. 10a. If all grid points on the ice sheet contains data then coverage is 1. All ~~timeseries~~ time series have close to full coverage during peak winter, where a campaign ensures full IW coverage of the ice sheet over a number of cycles. The coverage of the PROMICE product drops to $\sim$ 0.7 outside the campaigns with a low during summer months. ~~The lower panel of Fig. 10~~Figure 10b shows the mean of the reported standard deviation for each ~~map~~ mosaic in the time series. In general, when coverage is low the noise goes up and vice versa. The 6dOnly_1cycle is the ~~timeseries~~ time series with highest reported ~~noise level~~error estimate.

Figure 11 provides a spatial view of the ~~fraction of~~ temporal coverage of the time series. It shows the percentage of all mosaics that have data in ~~each~~ a given grid point for each of the time series. Blue colors indicate that a grid point rarely has data throughout the time series, while yellow indicates a temporal coverage close to 100%. A number of circumstances influence the temporal coverage: The more acquisitions cover a grid point, the more likely it is to have a pair where coherence is not lost. The number of acquisitions depends on the time of year, the location and the time span of the product (the PROMICE product includes more pairs than any of the three other time series). The temporal coverage also depends on how often coherence is lost leading to how often the processing fails.

All four time series have a large ~~blue~~ low-coverage area in the ~~ice sheet~~ ice-sheet interior, where SAR data in IW mode is rarely acquired as is evident from Fig. 2. The same explanation is true for the smaller triangular areas in the Melville Bay area and northern Greenland as well as the Scoresbysund area ~~.~~ (locations 1, 2, and 3 in Fig. 11a). However, the large ~~blue/green area~~ area with low coverage along the southeast ice sheet margin as well as an area in southern Greenland, one north of Rink Glacier in ~~West~~ west Greenland, and one in the Melville Bay area all have routine SAR IW acquisitions every 6 days ~~.~~ (locations 4, 5, 6, and 7 in Fig. 11 a). This will be discussed in the following.

The coverage and quality of each mosaic depend both on the SAR data coverage, the ~~amount of data~~ number of acquisitions going into each mosaic as well as on how the properties of the ice-sheet surface have changed between acquisitions (~~Section~~Sect. 5, ~~Section~~Sect. 4.4 and Fig. 2a). The PROMICE product has the best coverage of the time series in Table 4 (excluding All-pairsNoCull) (Fig. 10 and 11) as it includes all the pairs contained in both 12dOnly and 6dOnly. Figure 10a shows that most

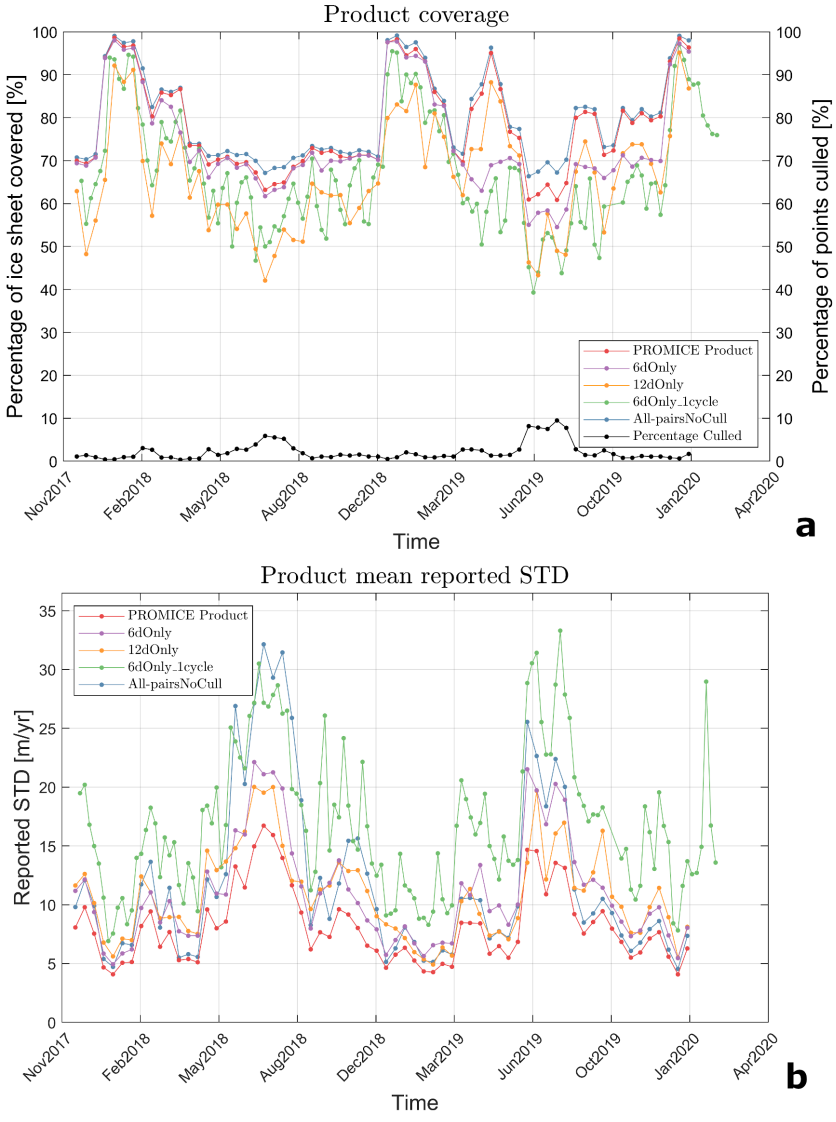

Figure 10. ~~Coverage and reported mean standard deviation~~a): The left axis shows the percentage of the ice sheet that is covered by data for each mosaic. Right axis: The lower blue curve shows the percentage of pixels that have been culled for the PROMICE ~~ice velocity~~ product ~~(All -2 cycles) is shown~~ using the procedure described in ~~red~~Sec. 4.5. b): The mean reported standard deviation for each mosaics.

often the 6dOnly has better coverage than the 12dOnly and for some extended periods of time, it is comparable to the PROMICE product. However, both 12dOnly and 6dOnly ~~timeseries~~ time series have periods with significant drops in coverage, while the PROMICE product still performs well. The difference in coverage is caused by differences in data acquisition and ice-sheet ~~surface properties~~surface properties.

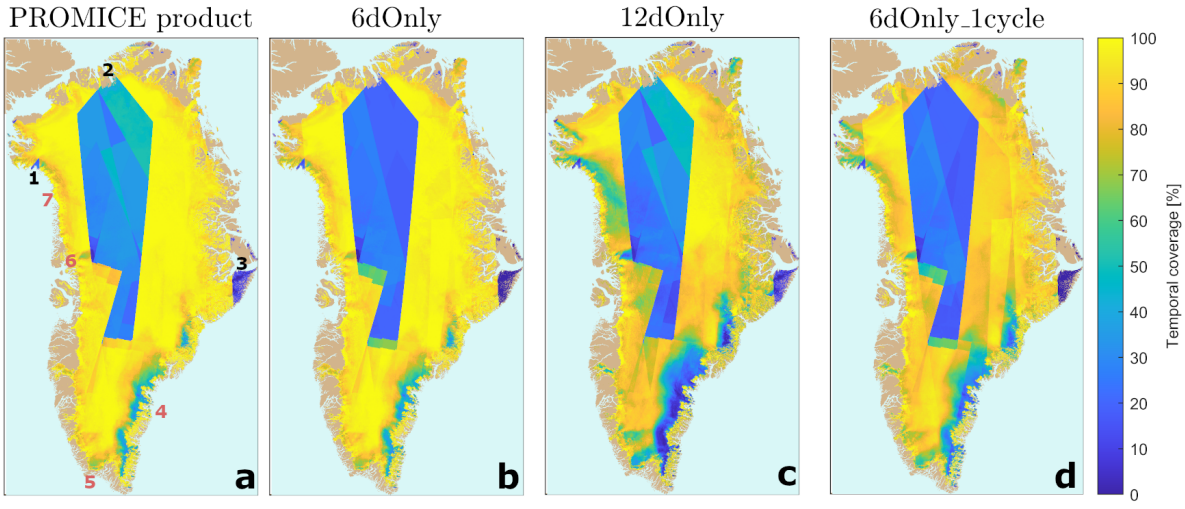

Figure 11. ~~Effect of including 6 and 12 day pairs on~~ Temporal coverage~~in~~ : Spatial view of the ~~mosaic~~percentage of all mosaics in that have data in a given grid point: a) The PROMICE ice velocity product b) 6dOnly time series c) 12dOnly ~~timeseries~~ time series and d) 6dOnly_1cycle ~~timeseries~~time series. The numbers in a) indicate the locations of the areas mentioned in Sec. 6: Areas where SAR in IW mode has not been acquired on a regular basis: 1, 2 and 3 refer to the triangular area in Melville Bay, north Greenland and the Scoresbysund area, respectively. Areas with low ice velocity coverage: 4, 5, 6 and 7 refer to the southeast ice sheet margin, small area in South Greenland, an area north of Rink Glacier and the Melville Bay area, respectively.

Not all tracks have both 12 day and 6 day coverage and often tracks in the interior are only covered by 12d pairs. This is revealed by the ~~lighter blue to green coloring~~ lower coverage of the interior for 12dOnly compared to ~~the dark blue for~~ 6dOnly in Fig. 11. 6dOnly has better coverage along the ice sheet margins compared to 12dOnly, because coherence is more likely to be preserved for shorter temporal baselines as discussed earlier in Sect. 3.1. The PROMICE product mosaics thus have better coverage than both 6dOnly and 12dOnly, because they each have coverage where the other does not. However, even using the short 6 day temporal baseline, some areas consistently have low coherence and therefore rarely have ice velocity coverage. The largest of these areas is the ~~Southeast~~ southeast ice sheet margin while the smaller areas include an area in southern Greenland, one north of Rink Glacier in ~~West~~ west Greenland, and one in the Melville Bay area (Fig. 11). The areas are apparent in all time series, but are most pronounced in the 12dOnly series as a longer temporal baseline increases the probability of changes to the surface properties due to precipitation and/or surface melt. The areas discussed here largely coincide with the regions identified as high accumulation percolation areas (HAPA) by Vandecrux et al. (2019) studying firn properties. HAPAs are areas on the ice sheet characterized by frequent precipitation events and surface melt-water that percolates into the firn -both processes ~~changing the properties observed by the radar~~leading to loss of coherence.

Figure 10 also shows the effect of performing the culling described in ~~Subsection~~Sect. 4.5 on the time series as a whole. The All-pairsNoCull is the PROMICE Product without culling. ~~Figure 10a shows that the~~ The effect on the coverage is minor

(Fig. 10a), however Fig. 10b shows that the average noise level is significantly reduced. ~~The points that are culled are thus also the points that the IPP processor assigns a high uncertainty to.~~

In the PROMICE ice velocity product each mosaic includes all possible ~~6 and 12 day~~ 6- and 12-day pairs within two consecutive Sentinel-1A cycles and the timestamps supplied with the product lists the timespan of the product (first and last date) as well as the midpoint time as specified in Table 1. This information is true for the mosaic, but not for a given grid point. This is due to:

- The SAR data (Fig. 2) is not acquired simultaneously over the GrIS as described in ~~Subsection~~Sect. 3.1.
- Different areas on the ice sheet are covered by a varying number of tracks/varying amount of data acquired at different times (also Fig. 2).
- Although data is acquired, the processor is unable to detect displacement for some pixels or larger areas due to loss of coherence or the processing of an image pair fails for various reasons and is therefore not included in the final mosaic.

Another point to keep in mind is that the mosaic is a weighted average of the processed pairs~~spanning 24 days~~. This means that although the product has a high temporal resolution, the time series will be smoothed and likely miss short lived (real) peaks in velocity for instance during summer.

The analysis from this section shows, that it is possible to provide a Greenland-wide ice velocity product with a higher temporal resolution than the PROMICE product (the 6dOnly_1cycle product), but also that this comes with the price of reduced spatial coverage and higher uncertainty. Creating a product spanning more than two Sentinel-1A cycles will have opposite effects. The two Sentinel-1A cycles choice for the PROMICE product is therefore a compromise between having reasonably high temporal resolution and good coverage and reducing noise.

7 Validation

We validate the PROMICE ice velocity product against in-situ GPS measurements from the PROMICE automatic weather stations (AWS) (van As et al., 2011; Fausto and van As, 2019) and perform an analysis over stable ground. Only a limited number of GPS measurements are available since the data ~~should~~ must overlap in time with the period of the PROMICE ice velocity product and have a ~~a~~ temporal resolution comparable to or higher than the PROMICE ice velocity product. Furthermore, the measurements are biased toward the slow moving parts of the ice sheet ablation zone. ~~We compare the PROMICE ice velocity product to in-situ GPS data from the PROMICE automatic weather stations (AWS) (van As et al., 2011).~~ Locations are displayed in Fig. 12.

PROMICE ~~AWS~~ AWSs measure a range of surface mass-balance components in the ablation zone of the ~~Greenland Ice Sheet~~GrIS. The stations are per design located in slow moving areas with an average flow generally lower than 100 m/yr (Fig. 12). The position of the AWS is measured every hour using a single frequency GPS receiver and a small ceramic patch active antenna. We use the freely available hourly positions ((Fausto and van As, 2019)) to calculate velocities using a workflow

similar to that described in GIScci-Consortium (2018): Daily positions of the GPS stations are calculated as a mean of the hourly positions for each day. The velocity components are estimated using a weighted linear regression for each of the 24-day time spans of the velocity mosaics using the daily positions. The weights are inversely proportional to the number of hourly measurements going into the estimate of a daily position in order to account for gaps in the data.

Scatter plots of the satellite derived PROMICE ice velocity product (magnitude, v_x and v_y components) vs. PROMICE GPS derived ice velocities are displayed in Fig. 13. The standard deviation of the difference between the GPS measurements and the satellite derived velocity (from here on referred to as the standard deviation) is calculated along with the mean difference (bias) between GPS and satellite velocity (see first line in Table 5). These values reflect not only the uncertainty of the satellite product but also that of the GPS derived velocity. The expected error of the satellite product is estimated to be 10-30 m/yr for individual pairs (GIScci-Consortium, 2013). The PROMICE product lies well within these bounds with a standard deviation and bias of 20 m/yr and -3 m/yr for the v_x ~~component~~ -component and 27 m/yr and -2 m/yr for the v_y ~~component~~-component, respectively. The larger standard deviation for the v_y component is expected: Due to the general ~~North-South~~ north-south orientation of the satellite tracks (Fig. 2), the v_y component is aligned roughly parallel to the azimuth direction (satellite flight path), and Sentinel-1 IW SLC images (see ~~Section~~ Sect. 3.1) have a much lower resolution in azimuth than in the range (line-of-)sight direction). We note that due to the ~~East~~roughly east/~~West~~ west orientation of most Greenland glaciers the velocity range of the y-component in our validation is notably smaller than that of the x-component.

We perform a similar analysis for the PROMICE product for the pixels over stable ground, where no movement is expected. All pixels on ice-free terrain from all mosaics (each spanning 24 days) in the time series are included, which totals to more than $142 \cdot 10^6$ pixels. The resulting values of the standard deviation and bias are 8 m/yr and 0.1 m/yr for the v_x-component and 12 m/yr and -0.6 m/yr for the v_y-component, respectively (see Table 6). The values of the standard deviation are less than half the values of the validation against GPS measurements, while the biases are significantly lower (in absolute value) and thus closer to zero. In this analysis, the standard deviation and bias are also largest for the v_y-component as discussed above.

Hvidberg et al. (2020) carried out a validation of many available satellite-derived ice-velocity products using an array of 63 GPS stations around EGRIP camp (75°38′ N, 35°60′ W) located on the Northeast Greenland Ice Stream. EGRIP camp is located in the ice-sheet accumulation zone, and Hvidberg et al. (2020) measured an average speed in the central flow line of 55 m/yr. The ice thus flows slowly at this location. The PROMICE ice velocity product was included in this analysis, and they found an average standard deviation of 6.6 m/yr for the products within the period September 13, 2016 to August 8, 2019. This is a significantly lower value of the standard deviation compared to what the validation against the PROMICE GPS observations shows, but similar to the analysis carried out on stable ground in ~~Subsection~~Sect. 5.2 (see Fig. 6). This difference is mainly due to two things: 1) In the accumulation zone, changes at the ice sheet surface are ~~mainly~~ most often due to snow fall and redistribution by wind. In contrast, in the ablation zone, where all the PROMICE GPS stations are located, the surface properties are influenced by several factors e.g. melt, high accumulation rates, and rain. This influences the coherence of image pairs and thereby increases uncertainty in the velocity product in these areas. 2) The uncertainty of the GPS measurements reported in Hvidberg et al. (2020) is lower compared to the PROMICE GPS observations. This is due to both the longer temporal baseline between measurements as well as the data acquisition time of 2-4 hours per

data point. The velocities derived from the PROMICE GPS observations may therefore carry a non negligible part of the uncertainty in the validation. None of the other products in the comparison by Hvidberg et al. (2020) have a similar high temporal resolution as the PROMICE ice velocity product. However, a 3-year average of the PROMICE ice velocity product was also included in the analysis and Hvidberg et al. (2020) found that it had a standard deviation (0.7 m/yr) similar to other offset/feature tracking products covering longer timespans like the annual maps from ESA CCI (Greenland Ice Sheet velocity maps from Sentinel-1 (Nagler et al., 2015)) and MEaSUREs Greenland Annual Ice Sheet Velocity Mosaics from SAR and Landsat, Version 1 [2015-2018] (Joughin et al., 2010), which have average values of 1.5 and 1.4 m/yr, respectively ~~(Hvidberg et al., 2020) Supp~~(supplementary material in Hvidberg et al., 2020). The standard deviation of the 3-year average of the PROMICE product is lower than for the annual maps, most likely because it includes more data. This is also a conclusion drawn by Hvidberg et al. (2020).

The 12dOnly and 6dOnly time series introduced in ~~Section~~Sect. 6 have similar standard deviations as the PROMICE product, when compared to the velocity derived from the PROMICE GPSs, whereas the higher temporal resolution product, 6dOnly_1cycle, has a significantly higher standard deviation. The PROMICE ice velocity product has the lowest standard deviation of the four. Using only 6 day pairs it is also possible to define a Greenland-wide product with a temporal resolution of 12 days, -the 6dOnly_1cycle product. It has the clear advantage of resolving the dynamics of the outlet glaciers even better, although this comes with the price of increased noise due to both the shorter temporal baseline and the geolocation bias as well as reduced coverage of each mosaic (Fig. 10a and b, Fig. 11 and Table 5). ~~It worth noticing that the outer most parts of the outlet glaciers still have reasonable coverage and for studying~~ For studies concerned with changes in fast flow ~~in these areas~~ the increased temporal resolution may outweigh the downsides. ~~The PROMICE ice velocity product as defined here provides a reasonable compromise between high coverage, temporal resolution, and noise.~~

The uncertainty reported in the ice velocity product is lower than the values we found during our validation against GPS. The average standard deviation found in Hvidberg et al. (2020) or the stable ground analysis is more comparable. The origin of some errors is such that the algorithm is unable to account for them. This is especially true for the spatially correlated errors caused by ionospheric scintillations (~~Section~~Sect. 5.4), which are not fully estimated by the error estimation algorithm (~~Section~~Sect. 5.6). A second issue is the distribution of the PROMICE AWSs biased towards the slow flowing parts of the ablation zone as well as the ~~uncertainly~~ uncertainty on the velocity estimates from these data.

For a time series of mosaics like the PROMICE ice velocity product, errors will vary both spatially and temporally due to the sources described in ~~Section~~Sect. 5 as well as to variations in data coverage (~~Subsection~~Sect. 4.4 and Fig. 2a). A ~~spatially better distributed set of validation data,~~ validation dataset which is not biased towards slow flowing areas in the ablation zone but is representative of a larger range of flow regimes and surface conditions would help assess whether the reported product errors capture this correctly. The analysis above, however, shows that the size of the product errors are as expected.

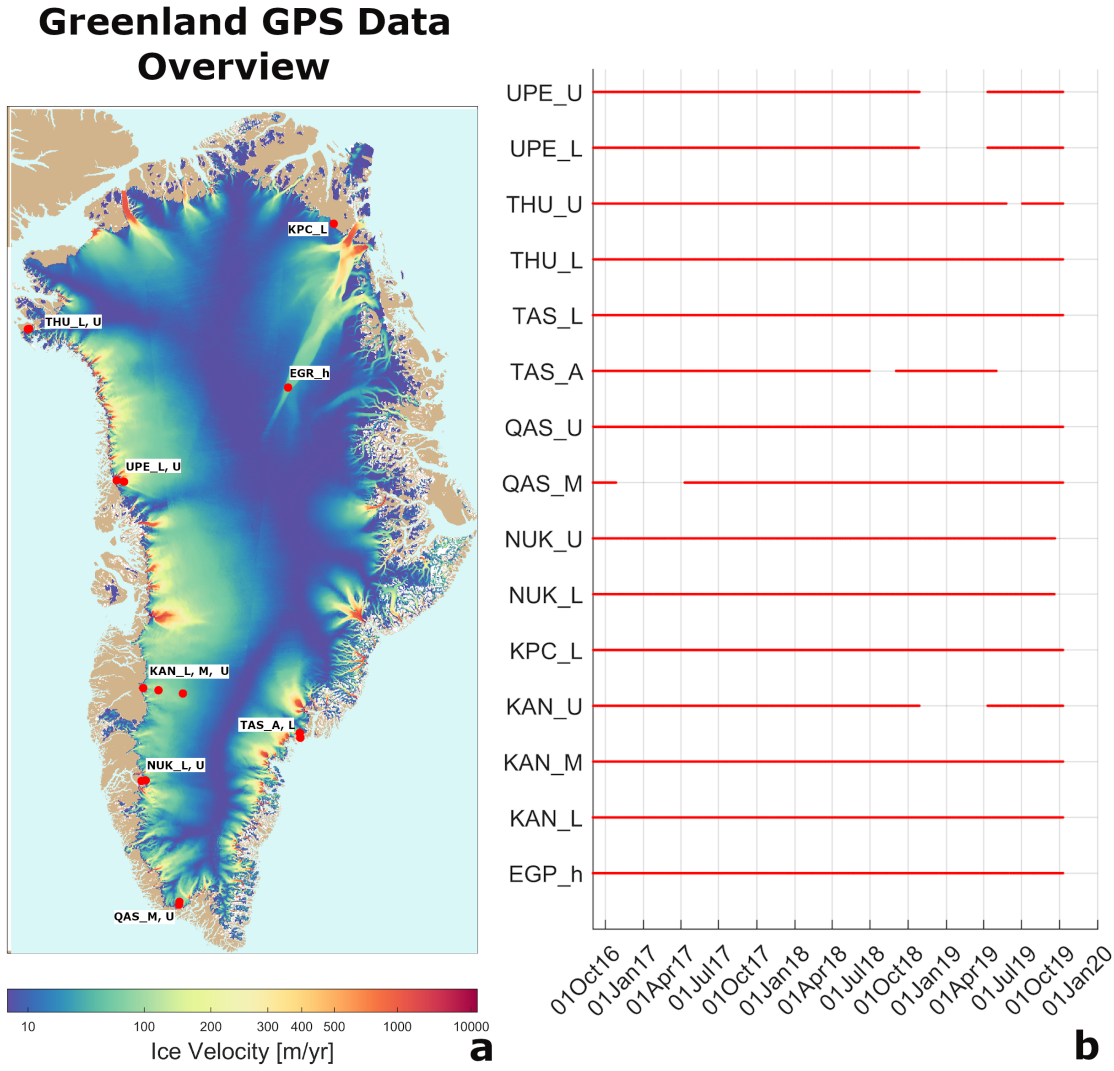

Figure 12. Overview of PROMICE GPS data: a) Locations of the PROMICE GPS stations on the ~~Greenland Ice Sheet~~GrIS. The ice velocity mosaic used as base layer is a 3 year average of all the PROMICE ice velocity maps spanning September 2016 to September 2019. b) List of PROMICE GPS stations used in the validation and their data coverage.

8 Living Data: Updates and Improvements

PROMICE will continue to distribute and update the PROMICE Ice Velocity product based on the Sentinel-1 data collected and released by ESA and the Copernicus programme. We aim to deliver a clean and homogenous data product and offer the possibility of user-interaction and addressing issues with the data product. Associated with PROMICE, we have a user-contributable dynamic web-based data archive (GitHub), which list known data quality issues [https://github.com/GEUS-

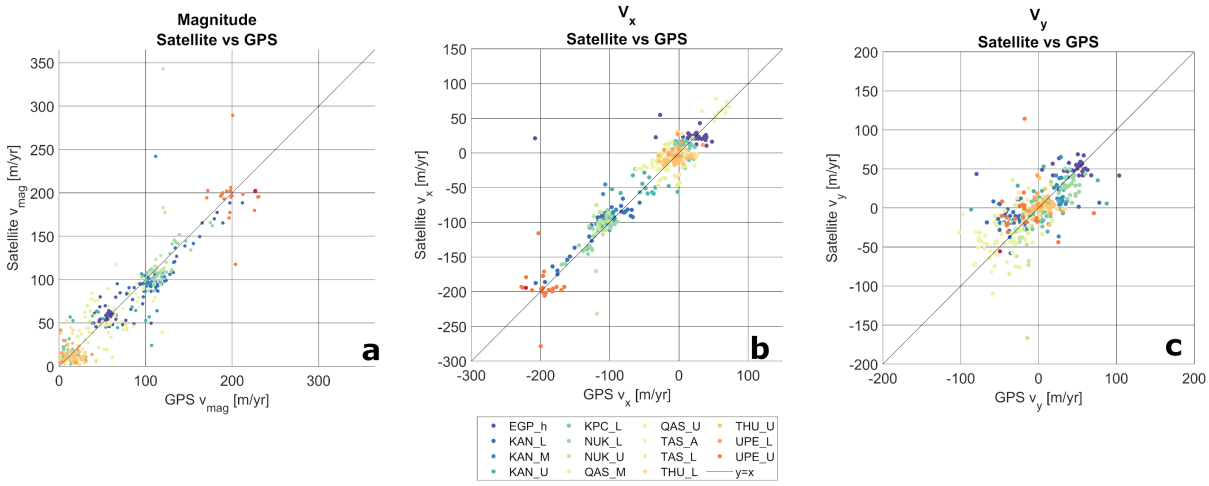

Figure 13. Scatterplots of PROMICE GPS ~~IV~~ ice velocity vs PROMICE ice velocity. a): Scatter plot of the magnitude of the velocity. b): Scatter plot of the v_x-component. c): Scatter plot of the v_y-component

Table 5. Statistics of the validation of the satellite ~~IV~~ ice velocity products using PROMICE GPS data.

Product	Magnitude		x-dir		y-dir	
	Std [m/yr]	Bias [m/yr]	Std [m/yr]	Bias [m/yr]	Std [m/yr]	Bias [m/yr]
PROMICE Product (All pairs)	19	4	20	-3	27	-2
6dOnly	22	0	21	-2	31	-1
12dOnly	19	4	20	-2	28	0
6dOnly_1cycle	34	9	31	-3	40	-2

PROMICE/Sentinel-1_Greenland_Ice_Velocity]. On the GitHub page, we also offer the opportunity for data users to add and document new issues. Documenting dataset issues is often simpler than correcting them and future dataset versions will implement fixes to any verified issues as soon as they are done. All fixed issues will be tagged as closed and remain visible for new users.

We encourage users who are working with Sentinel-1 and the PROMICE ice-velocity data to search the issue database and see if there are any known data issues relevant to their needs. We find it likely that there are issues unknown to us in the existing data and new issues may be found in the future data collection pipeline. We will do our best to improve the dataset with user-based help through the GitHub page.

Table 6. Statistics of the validation of the PROMICE product (spanning 24 days) over stable ground. Number of pixels included in the analysis: $> 142 \cdot 10^6$.

Product	Magnitude		x-dir		y-dir	
	Std [m/yr]	Bias [m/yr]	Std [m/yr]	Bias [m/yr]	Std [m/yr]	Bias [m/yr]
PROMICE Product (All pairs)	10	10	8	0.1	12	-0.6

9 Summary and Outlook

We have presented the PROMICE ice velocity product -a time series of GrIS wide velocity mosaics (September 2016 to present) based on Sentinel-1 SAR data. The product has a 500 m spatial- and 24 day temporal resolution and is produced in an operational setup using the IPP processor. A new mosaic is produced every 12 days and is made available within 10 days of the last included acquisition. During the winter campaigns, this lag is larger due to the amount of data to be processed. Validation against PROMICE AWS GPS data show that the standard deviation of the difference between the ice velocity product and the GPS data is 20 m/yr and 27 m/yr for v_x and v_y-component, respectively. This is within the expected uncertainty range of 10-30 m/yr (GIScci-Consortium, 2013). However, we expect the actual values pertaining to the PROMICE ice velocity product to be lower as the PROMICE AWS GPS data carry a non negligible part of the uncertainty. This is ~~also~~ indicated by the analysis carried out for pixels over stable ground, which showed a standard deviation of 8 m/yr and 12 m/yr for v_x and v_y-component, respectively as well as by the study of Hvidberg et al. (2020). Better spatially distributed validation data with low uncertainty would help assessing whether the processor captures the spatially and temporally varying uncertainty field correctly.

Ice velocities are retrieved by applying intensity offset-tracking to Sentinel-1 images acquired 6 and 12 days apart. The resulting velocity maps from all image pairs acquired during a 24-day period are temporally averaged and mosaicked to produce a consistent coverage. The processing chain is described in detail from the input data to the final outlier removal. We discuss the various error sources, which include biases and smoothly varying errors due to orbit and timing errors, noise-like errors due to changes in radar backscatter between radar acquisitions, and errors due to ionospheric scintillations. The error estimation approach is also described.

We show how the product coverage ~~vary~~ varies temporally and spatially in response to variations in SAR data acquisitions and seasonal changes in surface properties. The ~~Southeast~~ southeast GrIS margin has good Sentinel-1 SAR data coverage, but often has gaps in the mosaics due to changes in the surface properties caused by surface melt and high precipitation rates, which hinder velocity retrieval. Other areas, like the small triangular area in the Melville Bay area, have low coverage in the mosaics simply due to lack of SAR data.

The PROMICE Ice Velocity product will continue to update as long as the Sentinel-1 satellites are in operation. We will continue to make improvements to the product, and these updates will be posted at https://github.com/GEUS-PROMICE/Sentinel-1_Greenland_Ice_Velocity. Users are encouraged to add and document product issues or suggest improvements.

The PROMICE ice velocity product presented here was originally intended primarily to calculate ice discharge through marine-terminating glaciers of the GrIS as done in Mankoff et al. (2020). The PROMICE ice velocity product is thus less suited for studying very short-lived changes in the velocity structure, as observed in-situ by e.g. Bartholomew et al. (2012) and Ahlstrøm et al. (2013) or through higher frequency acquisitions/non-mosaic products of satellite imagery as done by e.g. Sundal et al. (2013) and Davison et al. (2020). By not mosaicking all the individual image pairs like we do for the PROMICE ice velocity product, a much higher temporal resolution over a limited region is possible. Yet, the spatially comprehensive and temporally consistent nature of the PROMICE ice velocity product makes it attractive also for longer term large-scale monitoring of the GrIS velocity structure and glacier dynamics as done by Vijay et al. (2019) and Solgaard et al. (2020).

10 Data availability

The PROMICE Ice Velocity product has DOI: https://doi.org/10.22008/promice/data/sentinel1icevelocity/greenlandicesheet and is available at https://dataverse01.geus.dk/dataverse/Ice_velocity. The product is updated regularly with a new mosaic every 12 days. Check out https://github.com/GEUS-PROMICE/Sentinel-1_Greenland_Ice_Velocity for updates and for posting issues.

Author contributions. AS and AK designed and produced the PROMICE ice velocity product. AK, JPMB and JD developed the processing software. RSF and KDM set up the data-curation framework. AS and AK prepared the manuscript with contributions from all co-authors.

Competing interests. Authors declare that they have no conflict of interest.

Acknowledgements. The authors thank the editor and Ben Davison and two anonymous reviewers for constructive comments and feedback. Ice velocity maps were produced as part of the Programme for Monitoring of the Greenland Ice Sheet (PROMICE) using Copernicus Sentinel-1 SAR images distributed by ESA, and were provided by the Geological Survey of Denmark and Greenland (GEUS) at http://www.promice.dk. AWS data from the Programme for Monitoring of the Greenland Ice Sheet (PROMICE) and the Greenland Analogue Project (GAP) were provided by the Geological Survey of Denmark and Greenland (GEUS) at http://www.promice.dk. Grounding line data are provided by the ESA Greenland Ice Sheet CCI project (www.esa-icesheets-greenland-cci.org).

References

Ahlstrøm, A. P., Andersen, S. B., Andersen, M. L., Machguth, H., Nick, F. M., Joughin, I., Reijmer, C. H., van de Wal, R. S. W., Merryman Boncori, J. P., Box, J. E., Citterio, M., van As, D., Fausto, R. S., and Hubbard, A.: Seasonal velocities of eight major marine-terminating outlet glaciers of the Greenland ice sheet from continuous in situ GPS instruments, Earth System Science Data, 5, 277–287, https://doi.org/10.5194/essd-5-277-2013, 2013.

Bartholomew, I., Nienow, P., Sole, A., Mair, D., Cowton, T., and King, M. A.: Short-term variability in Greenland Ice Sheet motion forced by time-varying meltwater drainage: Implications for the relationship between subglacial drainage system behavior and ice velocity, Journal of Geophysical Research: Earth Surface, 117, https://doi.org/https://doi.org/10.1029/2011JF002220, 2012.

Boncori, J. P. M., Andersen, M. L., Dall, J., Kusk, A., Kamstra, M., Andersen, S. B., Bechor, N., Bevan, S., Bignami, C., Gourmelen, N., and et al.: Intercomparison and Validation of SAR-Based Ice Velocity Measurement Techniques within the Greenland Ice Sheet CCI Project, Remote Sensing, 10, 929, https://doi.org/10.3390/rs10060929, http://dx.doi.org/10.3390/rs10060929, 2018.

Davison, B. J., Sole, A. J., Cowton, T. R., Lea, J. M., Slater, D. A., Fahrner, D., and Nienow, P. W.: Subglacial Drainage Evolution Modulates Seasonal Ice Flow Variability of Three Tidewater Glaciers in Southwest Greenland, Journal of Geophysical Research: Earth Surface, 125, e2019JF005 492, https://doi.org/https://doi.org/10.1029/2019JF005492, 2020.

de Lange, R., Luckman, A., and Murray, T.: Improvement of Satellite Radar Feature Tracking for Ice Velocity Derivation by Spatial Frequency Filtering, IEEE Transactions on Geoscience and Remote Sensing, 45, 2309–2318, https://doi.org/10.1109/TGRS.2007.896615, 2007.

De Zan, F.: Accuracy of Incoherent Speckle Tracking for Circular Gaussian Signals, IEEE Geoscience and Remote Sensing Letters, 11, 264–267, https://doi.org/10.1109/LGRS.2013.2255259, 2014.

De Zan, F. and Guarnieri, A. M.: TOPSAR: Terrain observation by progressive scans, IEEE Transactions on Geoscience and Remote Sensing, https://doi.org/10.1109/TGRS.2006.873853, 2006.

Fausto, R. and van As, D.: Programme for monitoring of the Greenland ice sheet (PROMICE): Automatic weather station data. Version: v03, Geological survey of Denmark and Greenland (GEUS)., https://doi.org/10.22008/promice/data/aws, 2019.

Gardner, A. S., Fahnestock, M. A., and Scambos, T. A.: ITS_LIVE Regional Glacier and Ice Sheet Surface Velocities., Data archived at National Snow and Ice Data Center, https://doi.org/10.5067/6II6VW8LLWJ7, 2019.

GIScci-Consortium: Comprehensive Error Characterisation Report for the Greenland Ice Sheet cci project of ESA's Climate Change Initiative, version 1.2, Tech. rep., European Space Agency, 2013.

GIScci-Consortium: Product Validation and Intercomparison Report (PVIR) for the Greenland Ice Sheet cci project of ESA's Climate Change Initiative, version 3.0, Tech. rep., European Space Agency, 2018.

Gisinger, C., Schubert, A., Breit, H., Garthwaite, M., Balss, U., Willberg, M., Small, D., Eineder, M., and Miranda, N.: In-Depth Verification of Sentinel-1 and TerraSAR-X Geolocation Accuracy Using the Australian Corner Reflector Array, IEEE Transactions on Geoscience and Remote Sensing, pp. 1–28, https://doi.org/10.1109/TGRS.2019.2961248, 2020.

Gomba, G.: Estimation of ionosphere-compensated azimuth ground motion with sentinel-1, Proceedings of the European Conference on Synthetic Aperture Radar, Eusar, pp. 87–90, 2018.

Gray, A., Mattar, K., Vachon, P., Bindschadler, R., Jezek, K., Forster, R., and Crawford, J.: InSAR results from the RADARSAT Antarctic Mapping Mission data: estimation of glacier motion using a simple registration procedure, in: IGARSS '98. Sensing and Managing the

Environment. 1998 IEEE International Geoscience and Remote Sensing. Symposium Proceedings. (Cat. No.98CH36174), pp. 1638–1640 vol.3, IEEE, https://doi.org/10.1109/IGARSS.1998.691662, http://ieeexplore.ieee.org/document/691662/, 1998.

Gray, A. L., Mattar, K. E., and Sofko, G.: Influence of Ionospheric Electron Density Fluctuations on Satellite Radar Interferometry, Geophysical Research Letters, https://doi.org/10.1029/2000GL000016, 2000.

Howat, I., Negrete, A., and Smith, B.: MEaSUREs Greenland Ice Mapping Project (GIMP) Digital Elevation Model, Version 1., NASA National Snow and Ice Data Center Distributed Active Archive Center, https://doi.org/doi: https://doi.org/10.5067/NV34YUIXLP9W, 2015.

Howat, I. M., Box, J. E., Ahn, Y., Herrington, A., and McFadden, E. M.: Seasonal variability in the dynamics of marine-terminating outlet glaciers in Greenland, Journal of Glaciology, 56, 601–613, https://doi.org/10.3189/002214310793146232, 2010.

Howat, I. M., Negrete, A., and Smith, B. E.: The Greenland Ice Mapping Project (GIMP) land classification and surface elevation data sets, The Cryosphere, 8, 1509–1518, https://doi.org/10.5194/tc-8-1509-2014, https://tc.copernicus.org/articles/8/1509/2014/, 2014.

Hvidberg, C. S., Grinsted, A., Dahl-Jensen, D., Khan, S. A., Kusk, A., Andersen, J. K., Neckel, N., Solgaard, A., Karlsson, N. B., Kjær, H. A., and Vallelonga, P.: Surface velocity of the Northeast Greenland Ice Stream (NEGIS): assessment of interior velocities derived from satellite data by GPS, The Cryosphere, 14, 3487–3502, https://doi.org/10.5194/tc-14-3487-2020, 2020.

Joughin, I.: Ice-sheet velocity mapping: a combined interferometric and speckle-tracking approach, Annals of Glaciology, 34, 195–201, https://doi.org/10.3189/172756402781817978, 2002.

Joughin, I.: MEaSUREs Greenland Annual Ice Sheet Velocity Mosaics from SAR and Landsat, Version 2., Boulder, Colorado USA. NASA National Snow and Ice Data Center Distributed Active Archive Center., https://doi.org/10.5067/TZZDYD94IMJB, 2020a.

Joughin, I.: MEaSUREs Greenland Monthly Ice Sheet Velocity Mosaics from SAR and Landsat, Version 2., Boulder, Colorado USA. NASA National Snow and Ice Data Center Distributed Active Archive Center., https://doi.org/0.5067/11MJZGPBK3ZF, 2020b.

Joughin, I.: MEaSUREs Greenland Quarterly Ice Sheet Velocity Mosaics from SAR and Landsat, Version 2, Boulder, Colorado USA. NASA National Snow and Ice Data Center Distributed Active Archive Center., https://doi.org/10.5067/3ZMCUIFDYJG4, 2020c.

Joughin, I., Smith, B. E., Howat, I. M., Scambos, T., and Moon, T.: Greenland flow variability from ice-sheet-wide velocity mapping, Journal of Glaciology, 56, 415–430, https://doi.org/10.3189/002214310792447734, 2010.

Joughin, I., Smith, B. E., and Howat, I.: Greenland Ice Mapping Project: ice flow velocity variation at sub-monthly to decadal timescales, The Cryosphere, 12, 2211–2227, https://doi.org/10.5194/tc-12-2211-2018, 2018.

Joughin, L. R., Kwok, R., and Fahnestock, M. A.: Interferometric estimation of three-dimensional ice-flow using ascending and descending passes, IEEE Transactions on Geoscience and Remote Sensing, https://doi.org/10.1109/36.655315, 1998.

Kusk, A., Boncori, J., and Dall, J.: An automated system for ice velocity measurement from SAR, in: Proceedings of the 12th European Conference on Synthetic Aperture Radar (EUSAR 2018), Proceedings of the European Conference on Synthetic Aperture Radar, pp. 929–932, VDE Verlag, 2018.

Liao, H., Meyer, F. J., Scheuchl, B., Mouginot, J., Joughin, I., and Rignot, E.: Ionospheric correction of InSAR data for accurate ice velocity measurement at polar regions, Remote Sensing of Environment, 209, 166 – 180, https://doi.org/https://doi.org/10.1016/j.rse.2018.02.048, http://www.sciencedirect.com/science/article/pii/S0034425718300580, 2018.

Maier, N., Humphrey, N., Harper, J., and Meierbachtol, T.: Sliding dominates slow-flowing margin regions, Greenland Ice Sheet, Science Advances, 5, https://doi.org/10.1126/sciadv.aaw5406, 2019.

Mankoff, K. D., Solgaard, A., Colgan, W., Ahlstrøm, A. P., Khan, S. A., and Fausto, R. S.: Greenland Ice Sheet solid ice discharge from 1986 through March 2020, Earth System Science Data, 12, 1367–1383, https://doi.org/10.5194/essd-12-1367-2020, 2020.

Mattar, K. E. and Gray, A. L.: Reducing ionospheric electron density errors in satellite radar interferometry applications, Canadian Journal of Remote Sensing, 28, 593–600, https://doi.org/10.5589/m02-051, 2002.

Miranda, N.: Definition of the TOPS SLC deramping function for products generated by the S-1 IPF (Technical Note COPE-GSEG-EOPG-TN-14-0025, Issue 1, Rev. 3), Tech. rep., European Space Agency, 2017.

Moon, T., Joughin, I., Smith, B., van den Broeke, M. R., van de Berg, W. J., Noël, B., and Usher, M.: Distinct patterns of seasonal Greenland glacier velocity, Geophysical Research Letters, 41, 7209–7216, https://doi.org/https://doi.org/10.1002/2014GL061836, 2014.

Moon, T. A., Gardner, A. S., Csatho, B., Parmuzin, I., and Fahnestock, M. A.: Rapid Reconfiguration of the Greenland Ice Sheet Coastal Margin, Journal of Geophysical Research: Earth Surface, 125, e2020JF005 585, https://doi.org/https://doi.org/10.1029/2020JF005585, 2020.

Mouginot, J., Bjørk, A. A., Millan, R., Scheuchl, B., and Rignot, E.: Insights on the Surge Behavior of Storstrømmen and L. Bistrup Bræ, Northeast Greenland, Over the Last Century, Geophysical Research Letters, 45, 11,197–11,205, https://doi.org/https://doi.org/10.1029/2018GL079052, 2018.

Mouginot, J., Rignot, E., Millan, R., and Wood, M.: Annual Ice Velocity of the Greenland Ice Sheet (1972-1990), Dryad, Dataset., https://doi.org/10.7280/D1MM37, 2019a.

Mouginot, J., Rignot, E., Scheuchl, B., Millan, R., and Wood, M. .: Annual Ice Velocity of the Greenland Ice Sheet (1991-2000), Dryad, Dataset., https://doi.org/10.7280/D1GW91, 2019b.

Mouginot, J., Rignot, E., Scheuchl, B., Wood, M., and Millan, R.: Annual Ice Velocity of the Greenland Ice Sheet (2001-2010), Dryad, Dataset., https://doi.org/10.7280/D1595V, 2019c.

Mouginot, J., Rignot, E., Scheuchl, B., Wood, M., and Millan, R.: Annual Ice Velocity of the Greenland Ice Sheet (2010-2017), Dryad, Dataset., https://doi.org/10.7280/D11H3X, 2019d.

Nagler, T., Rott, H., Hetzenecker, M., Wuite, J., and Potin, P.: The Sentinel-1 mission: New opportunities for ice sheet observations, Remote Sensing, https://doi.org/10.3390/rs70709371, 2015.

Padman, L., Siegfried, M. R., and Fricker, H. A.: Ocean Tide Influences on the Antarctic and Greenland Ice Sheets, Reviews of Geophysics, 56, 142–184, https://doi.org/https://doi.org/10.1002/2016RG000546, https://agupubs.onlinelibrary.wiley.com/doi/abs/10.1002/2016RG000546, 2018.

Peter, H., Jäggi, A., Fernández, J., Escobar, D., Ayuga, F., Arnold, D., Wermuth, M., Hackel, S., Otten, M., Simons, W., Visser, P., Hugentobler, U., and Féménias, P.: Sentinel-1A – First precise orbit determination results, Advances in Space Research, 60, 879 – 892, https://doi.org/https://doi.org/10.1016/j.asr.2017.05.034, http://www.sciencedirect.com/science/article/pii/S0273117717303794, 2017.

Reeh, N., Mayer, C., Olesen, O. B., Christensen, E. L., and Thomsen, H. H.: Tidal movement of Nioghalvfjerdsfjorden glacier, northeast Greenland: observations and modelling, Annals of Glaciology, 31, 111–117, https://doi.org/10.3189/172756400781820408, 2000.

Rignot, E. and Kanagaratnam, P.: Changes in the Velocity Structure of the Greenland Ice Sheet, Science, 311, 986–990, https://doi.org/10.1126/science.1121381, 2006.

Rosenau, R., Scheinert, M., and Dietrich, R.: A processing system to monitor Greenland outlet glacier velocity variations at decadal and seasonal time scales utilizing the Landsat imagery, Remote Sensing of Environment, 169, 1 – 19, https://doi.org/https://doi.org/10.1016/j.rse.2015.07.012, 2015.

Schubert, A., Miranda, N., Geudtner, D., and Small, D.: Sentinel-1A/B combined product geolocation accuracy, Remote Sensing, 9, 607, https://doi.org/10.3390/rs9060607, 2017.

Shepherd, A., Ivins, E., Rignot, E., Smith, B., van den Broeke, M., Velicogna, I., Whitehouse, P., Briggs, K., Joughin, I., Krinner, G., Nowicki, S., Payne, T., Scambos, T., Schlegel, N., Geruo, A., Agosta, C., Ahlstrøm, A., Babonis, G., Barletta, V. R., Bjørk, A. A., Blazquez, A., Bonin, J., Colgan, W., Csatho, B., Cullather, R., Engdahl, M. E., Felikson, D., Fettweis, X., Forsberg, R., Hogg, A. E., Gallee, H., Gardner, A., Gilbert, L., Gourmelen, N., Groh, A., Gunter, B., Hanna, E., Harig, C., Helm, V., Horvath, A., Horwath, M., Khan, S., Kjeldsen, K. K., Konrad, H., Langen, P. L., Lecavalier, B., Loomis, B., Luthcke, S., McMillan, M., Melini, D., Mernild, S., Mohajerani, Y., Moore, P., Mottram, R., Mouginot, J., Moyano, G., Muir, A., Nagler, T., Nield, G., Nilsson, J., Noël, B., Otosaka, I., Pattle, M. E., Peltier, W. R., Pie, N., Rietbroek, R., Rott, H., Sørensen, L. S., Sasgen, I., Save, H., Scheuchl, B., Schrama, E., Schröder, L., Seo, K.-W., Simonsen, S. B., Slater, T., Spada, G., Sutterley, T., Talpe, M., Tarasov, L., Jan van de Berg, W., van der Wal, W., van Wessem, M., Vishwakarma, B. D., Wiese, D., Wilton, D., Wagner, T., Wouters, B., and Wuite, J.: Mass balance of the Greenland Ice Sheet from 1992 to 2018, Nature, 2019.

Sole, A. J., Mair, D. W. F., Nienow, P. W., Bartholomew, I. D., King, M. A., Burke, M. J., and Joughin, I.: Seasonal speedup of a Greenland marine-terminating outlet glacier forced by surface melt–induced changes in subglacial hydrology, Journal of Geophysical Research: Earth Surface, 116, https://doi.org/https://doi.org/10.1029/2010JF001948, 2011.

Solgaard, A. and Kusk, A.: Greenland Ice Velocity from Sentinel-1 Edition 2, https://doi.org/10.22008/promice/data/sentinel1icevelocity/greenlandicesheet 2021.

Solgaard, A. M., Simonsen, S. B., Grinsted, A., Mottram, R., Karlsson, N. B., Hansen, K., Kusk, A., and Sørensen, L. S.: Hagen Bræ: A Surging Glacier in North Greenland—35 Years of Observations, Geophysical Research Letters, 47, e2019GL085 802, https://doi.org/https://doi.org/10.1029/2019GL085802, 2020.

Strozzi, T., Luckman, A., Murray, T., Wegmüller, U., and Werner, C. L.: Glacier motion estimation using SAR offset-tracking procedures, IEEE Transactions on Geoscience and Remote Sensing, https://doi.org/10.1109/TGRS.2002.805079, 2002.

Sundal, A., Shepherd, A., van den Broeke, M., Van Angelen, J., Gourmelen, N., and Park, J.: Controls on short-term variations in Greenland glacier dynamics, Journal of Glaciology, 59, 883–892, https://doi.org/10.3189/2013JoG13J019, 2013.

Thomas, R. H., Csathó, B. M., Gogineni, S., Jezek, K. C., and Kuivinen, K.: Thickening of the western part of the Greenland ice sheet, Journal of Glaciology, 44, 653–658, https://doi.org/10.3189/S002214300000215X, 1998.

van As, D., Fausto, R. S., and PROMICE project team, .: Programme for Monitoring of the Greenland Ice Sheet (PROMICE): first temperature and ablation records, GEUS Bulletin, 23, 73–76, 2011.

Vandecrux, B., MacFerrin, M., Machguth, H., Colgan, W. T., van As, D., Heilig, A., Stevens, C. M., Charalampidis, C., Fausto, R. S., Morris, E. M., Mosley-Thompson, E., Koenig, L., Montgomery, L. N., Miège, C., Simonsen, S. B., Ingeman-Nielsen, T., and Box, J. E.: Firn data compilation reveals widespread decrease of firn air content in western Greenland, The Cryosphere, 13, 845–859, https://doi.org/10.5194/tc-13-845-2019, 2019.

Vijay, S., Khan, S. A., Kusk, A., Solgaard, A. M., Moon, T., and Bjørk, A. A.: Resolving Seasonal Ice Velocity of 45 Greenlandic Glaciers With Very High Temporal Details, Geophysical Research Letters, 46, 1485–1495, https://doi.org/https://doi.org/10.1029/2018GL081503, 2019.

Westerweel, J. and Scarano, F.: Universal outlier detection for PIV data, Experiments in Fluids, 39, 1096–1100, https://doi.org/10.1007/s00348-005-0016-6, 2005.